

DTIC FILE COPY

12

NSWC TR 87-96

AD-A180 901

**NOTES ON A PARACHUTE OPENING FORCE  
ANALYSIS APPLIED TO A VERTICAL  
TOWARD-THE-EARTH TRAJECTORY**

BY WILLIAM P. LUDTKE

UNDERWATER SYSTEMS DEPARTMENT

28 MAY 1987

DTIC  
ELECTE  
JUN 09 1987  
S D

Approved for public release, distribution is unlimited.



**NAVAL SURFACE WEAPONS CENTER**

Dahlgren, Virginia 22448-5000 • Silver Spring, Maryland 20903-5000

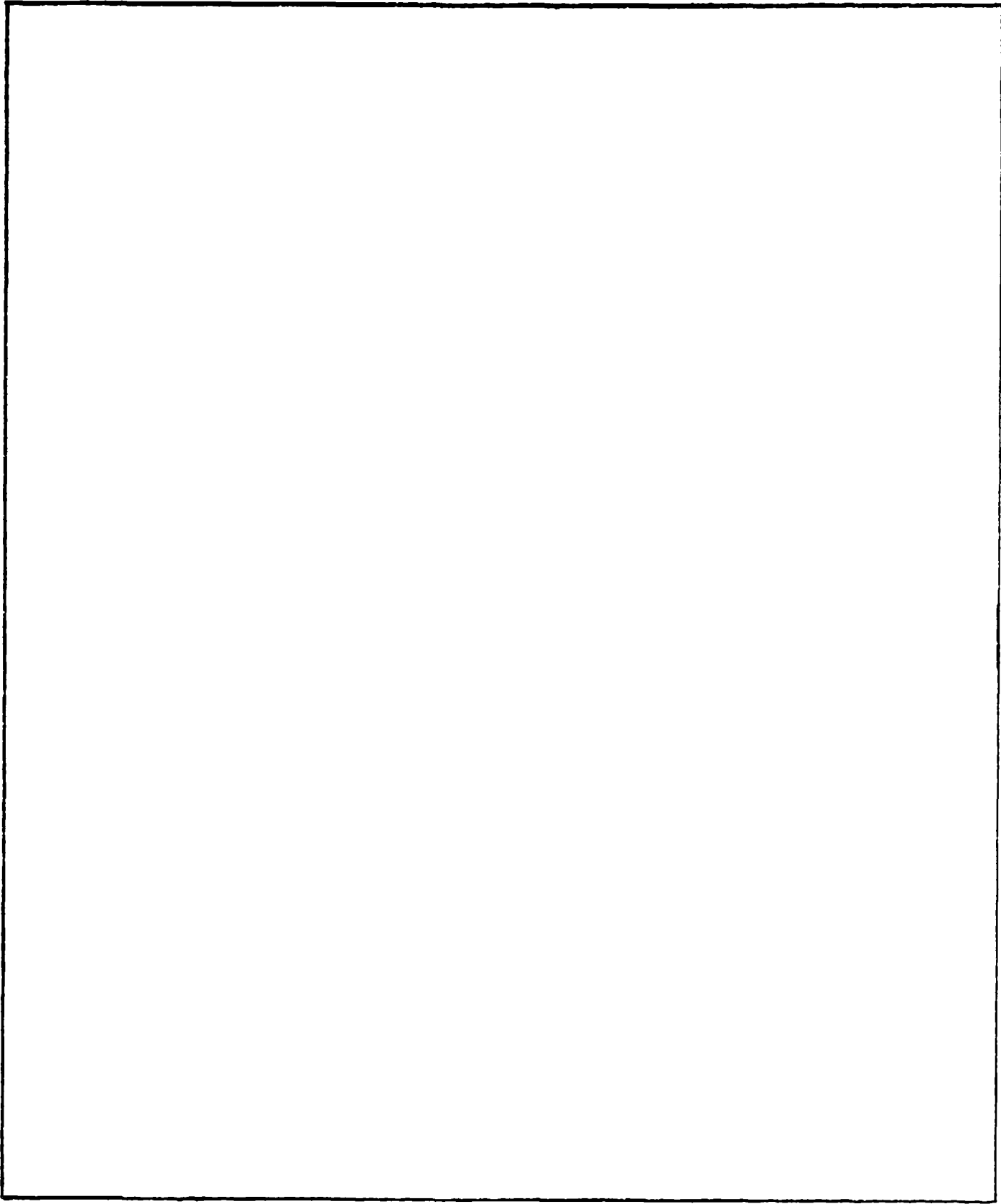
87 6 5 019

REPORT DOCUMENTATION PAGE

1a. REPORT SECURITY CLASSIFICATION UNCLASSIFIED			1b. RESTRICTIVE MARKINGS		
2a. SECURITY CLASSIFICATION AUTHORITY			3. DISTRIBUTION / AVAILABILITY OF REPORT Approved for public release; distribution is unlimited.		
2b. DECLASSIFICATION / DOWNGRADING SCHEDULE			4. PERFORMING ORGANIZATION REPORT NUMBER(S) NSWC TR 87-96		
4. PERFORMING ORGANIZATION REPORT NUMBER(S)			5. MONITORING ORGANIZATION REPORT NUMBER(S)		
6a. NAME OF PERFORMING ORGANIZATION Naval Surface Weapons Center		6b. OFFICE SYMBOL (If applicable) (U13)	7a. NAME OF MONITORING ORGANIZATION		
6c. ADDRESS (City, State, and ZIP Code) 10901 New Hampshire Ave. Silver Spring, MD 20903-5000			7b. ADDRESS (City, State, and ZIP Code)		
8a. NAME OF FUNDING / SPONSORING ORGANIZATION		8b. OFFICE SYMBOL (If applicable)	9. PROCUREMENT INSTRUMENT IDENTIFICATION NUMBER		
8c. ADDRESS (City, State, and ZIP Code)			10. SOURCE OF FUNDING NUMBERS		
		PROGRAM ELEMENT NO. N/A	PROJECT NO. 4U81VA	TASK NO. N/A	WORK UNIT ACCESSION NO. N/A
11. TITLE (Include Security Classification) NOTES ON A PARACHUTE OPENING FORCE ANALYSIS APPLIED TO A VERTICAL TOWARD-THE-EARTH TRAJECTORY					
12. PERSONAL AUTHOR(S) WILLIAM P. LUDTKE					
13a. TYPE OF REPORT Final		13b. TIME COVERED FROM 1986 TO 1987	14. DATE OF REPORT (Year, Month, Day) 87/5/28	15. PAGE COUNT	
16. SUPPLEMENTARY NOTATION					
17. COSATI CODES			18. SUBJECT TERMS (Continue on reverse if necessary and identify by block number)		
FIELD	GROUP	SUB-GROUP			
01	03		Vertical Deployment Opening Shock Vertical Inflation Time Calculation Methods Parachute Technology Limiting Ballistic Mass Ratio		
19. ABSTRACT (Continue on reverse if necessary and identify by block number) Recovery of payloads from high altitude often requires the deployment of parachutes on trajectories that are essentially vertical and toward the earth. The parachute opening shock force developed by a parachute deployed in this manner exceeds the opening shock force of the same parachute system deployed horizontally at the same altitude and velocity. As the deployment trajectory angle varies from horizontal to vertical; the opening shock force increases to a maximum. Hence, the vertical trajectory has special significance. This report develops an analysis to permit the calculation of opening shock forces in vertical deployment. The validity of the rule of thumb that "the vertical deployment opening shock force exceeds the horizontal shock force by one "g" is tested, and criteria are developed.  Examples are used to demonstrate applications of the approach, and a method of calculating the inflation time of Solid Cloth parachutes in vertical fall developed.					
20. DISTRIBUTION / AVAILABILITY OF ABSTRACT <input type="checkbox"/> UNCLASSIFIED/UNLIMITED <input checked="" type="checkbox"/> SAME AS RPT. <input type="checkbox"/> DTIC USERS			21. ABSTRACT SECURITY CLASSIFICATION UNCLASSIFIED		
22a. NAME OF RESPONSIBLE INDIVIDUAL WILLIAM P. LUDTKE			22b. TELEPHONE (Include Area Code) 202/394-1705	22c. OFFICE SYMBOL U13	

UNCLASSIFIED

SECURITY CLASSIFICATION OF THIS PAGE



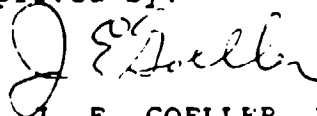
FOREWORD

Recovery of payloads from high altitude often requires the deployment of parachutes on trajectories that are essentially vertical and toward the earth. The parachute opening shock force developed by a parachute deployed in this manner exceeds the opening shock force of the same parachute system deployed horizontally at the same altitude and velocity. As the deployment trajectory angle varies from horizontal to vertical, the opening shock force increases to a maximum. Hence, the vertical trajectory has special significance. This report develops an analysis to permit the calculation of opening shock forces in vertical deployment. The validity of the rule of thumb that "the vertical deployment opening shock force exceeds the horizontal shock force by one "g" is tested, and criteria are developed.

Examples are used to demonstrate applications of the approach and a method of calculating the inflation time of solid cloth parachutes in vertical fall is developed.

The author wishes to express his appreciation to Mr. Hensel Brown of the Strategic Systems Department for his valuable assistance. Mr. Brown developed the computer programs and conducted numerous background calculations for this report.

Approved by:



Dr. J. E. GOELLER, Head  
Underwater Weapons Division



iii/iv

Accession For	
NTIS CR&I	<input checked="" type="checkbox"/>
DTIC TAB	<input type="checkbox"/>
Unannounced	<input type="checkbox"/>
Justification	
By	
Distribution/	
Availability Codes	
Dist	Avail and for special
A-1	

CONTENTS

	<u>Page</u>
INTRODUCTION . . . . .	1
APPROACH . . . . .	3
SUMMARY AND CONCLUSIONS. . . . .	23
REFERENCES . . . . .	25
APPENDIX A--AIAA PAPER NO. 73-477, "A TECHNIQUE FOR THE CALCULATION OF THE OPENING-SHOCK FORCES FOR SEVERAL TYPES OF SOLID CLOTH PARACHUTES". . . . .	A-1
APPENDIX B--A GUIDE FOR THE USE OF APPENDIX A. . . . .	B-1

## ILLUSTRATIONS

<u>Figure</u>		<u>Page</u>
1	VERTICAL TRAJECTORY POINT MASS FORCE SYSTEM . . . . .	3
2	VARIATION OF THE INFLATION REFERENCE TIME AS A FUNCTION OF SYSTEM WEIGHT FOR THE FLAT CIRCULAR SOLID CLOTH PARACHUTE OF EXAMPLE ONE. . . . .	9
3	OPENING SHOCK FORCE IN THE HORIZONTAL AND VERTICAL DEPLOYMENT MODES AS A FUNCTION OF INFLATION REFERENCE TIME FOR A SYSTEM WEIGHT OF 200 POUNDS. . . . .	18
4	OPENING SHOCK FORCES AT THE INFLATION REFERENCE TIME $t=t_0$ IN THE HORIZONTAL AND VERTICAL DEPLOYMENT MODES AS A FUNCTION OF INFLATION REFERENCE TIME FOR A SYSTEM WEIGHT OF 2000 POUNDS . . . . .	20

TABLES

<u>Table</u>		<u>Page</u>
1	INSTANTANEOUS DRAG AREA, VELOCITY, OPENING SHOCK FORCE, AND DISTANCE OF FALL OF A PARACHUTE DEPLOYED IN VERTICAL FALL . . . . .	14
2	SUMMARY OF THE FLAT CIRCULAR SOLID CLOTH PARACHUTE VERTICAL TRAJECTORY CALCULATIONS FOR A VALUE OF TIME INCREMENT $dt=t_0/100000$ . . . . .	16

## INTRODUCTION

Parachutes are used to reduce the impact velocity of many falling objects. Often the parachute systems are initiated while moving in a trajectory which is parallel to the earth's surface. Many methods of calculating parachute opening shock force use the horizontal attitude as a basis for analysis. However, in the recovery of systems which have been allowed to free fall from high altitudes, the trajectory deviates markedly from the horizontal and approaches the vertical direction. The opening shock force of a vertically toward-the-earth deployed system is known to exceed the horizontal deployment shock force for the identical system and operational altitude and velocity.

Vertical trajectories are of special interest since the opening shock force is a maximum value. The purpose of this report is to develop a method for calculating the drag area, velocity and shock factor profiles, opening shock force, time of occurrence of the shock force during canopy inflation, and the distance of fall for parachutes deployed in a vertical toward-the-earth trajectory. This report is an extension of Reference 1, NSWC TR86-142, "Notes on a Generic Parachute Opening Force Analysis", which describes a technique of calculating the opening shock force of several types of horizontally deployed parachutes. In the interest of clarity readers should familiarize themselves with Reference 1, as it is to be used extensively in this report.

A method of calculating the inflation time of solid cloth parachutes in vertical fall is developed and horizontal and vertical inflation times for identical deployment conditions are compared. Criteria required for inflation time analysis of other types of parachutes are presented.

There is a rule of thumb used in calculating the opening shock force of vertically deployed parachutes. The rule states that "the vertical mode opening shock force is equal to the horizontal mode opening shock force, plus one g". Examples demonstrate that the vertical deployment mode inflation reference time is less than the horizontal deployment mode inflation reference time for the same system, velocity and altitude. The theory indicates that the vertical deployment mode opening shock forces exceed the rule of thumb.

## APPROACH

The analysis is based upon the application of Newton's second law of motion to particle trajectories of inflating parachutes in the horizontal and toward-the-earth vertical modes. Equations for the horizontal deployment of parachutes with dynamic drag-area signatures of the form  $C_D S / C_{D0} S_0 = (1 - \tau) (t/t_0)^j + \tau$  were developed in Reference 1. The same dynamic drag-area signatures are to be incorporated into the vertical deployment analysis. The exponent  $j$  determines the type of parachute. A value of  $j=1$  is indicative of geometrically porous ribbon and ring slot types of canopies. Solid cloth parachutes have a value of  $j=6$ .

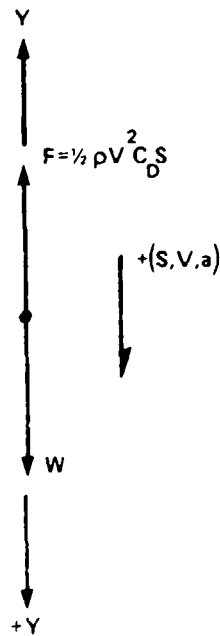


FIGURE 1. VERTICAL TRAJECTORY POINT MASS FORCE SYSTEM

$$\Sigma F_y = m a_y$$

$$W - \frac{1}{2} \rho V^2 C_D S = \frac{W}{g} \frac{dV}{dt} = \frac{W}{g} V \frac{dV}{dS} \quad (1)$$

## DEVELOPMENT OF THE VELOCITY - TIME EQUATIONS

With reference to Figure 1.

$$dV = \left( g - \frac{g\rho V^2 C_D S}{2W} \right) dt$$

$$\frac{C_D S}{C_D S_0} = (1 - \tau) \left( \frac{t}{t_0} \right)^j + \tau \quad (2)$$

$$dV = \left( g - \frac{g\rho V^2 C_D S_0}{2W} \times \frac{V_s t_0}{V_s t_0} \left( (1 - \tau) \left( \frac{t}{t_0} \right)^j + \tau \right) \right) dt$$

where the quantity  $2W/(\rho g V_s t_0 C_D S_0)$  has been shown in Reference 1 to be a ballistic mass ratio scale factor.

$$\text{Let } M = \frac{2W}{\rho g V_s t_0 C_D S_0} \quad (3)$$

$$\sum_{V=V_s}^V dV = \sum_{t=0}^t \left( g - \frac{V^2}{M V_s t_0} \left( (1 - \tau) \left( \frac{t}{t_0} \right)^j + \tau \right) \right) dt \quad (4)$$

## DEVELOPMENT OF THE DISTANCE-TIME EQUATION.

Application of the variable dynamic drag area and ballistic mass ratio equations to the velocity distance form of equation (1) yields.

$$\sum_{s=0}^s dS = \sum_{V=V_s}^V \frac{V dV}{\left( g - \frac{V^2}{M V_s t_0} \left( (1 - \tau) \left( \frac{t}{t_0} \right)^j + \tau \right) \right)} \quad (5)$$

At any instant during the inflation process the shock factor has been shown to be:

$$\chi_i = \left( \frac{V}{V_s} \right)^2 \frac{C_D S}{C_D S_0} \quad (6)$$

and the instantaneous shock force is:

$$F_i = X_i F_s \quad (7)$$

where  $F_s$  is the steady-state drag force of the fully open parachute at the line stretch velocity,  $V_s$ .

$$F_s = \frac{1}{2} \rho V_s^2 C_D S_0 \quad (8)$$

The opening shock performance in the vertical and horizontal deployment modes shall be demonstrated by examples.

Example 1: Compare the horizontal and vertical deployment mode opening shock forces for a flat circular solid cloth parachute of 35 feet  $D_0$  diameter and 30 gores. Deployment conditions are:

- a. System weight = 200 lb.
- b. Density altitude = 3,000 ft.
- c. Line stretch velocity = 340 fps.
- d. Drag coefficient = 0.75
- e. Dynamic drag area exponent,  $j=6$
- f. Initial drag area,  $r=0$

#### HORIZONTAL OPENING SHOCK FORCE

- a. Parachute surface area

$$S_0 = \frac{\pi}{4} D_0^2$$

$$S_0 = \frac{\pi}{4} (35)^2$$

$$S_0 = 962.1 \text{ ft}^2$$

b. Parachute drag area:

$$C_D S_o = 0.75 \times 962.1$$

$$C_D S_o = 721.6 \text{ ft}^2$$

c. Air density,  $\rho = 0.0021753 \text{ slugs/ft}^3$

d. Steady-state drag force

$$F_s = \frac{1}{2} \rho V_s^2 C_D S_o$$

$$F_s = \frac{1}{2} \times 0.0021753 (340)^2 721.6$$

$$F_s = 90726.7 \text{ lb.}$$

e. In order to determine the ballistic mass ratio, the inflation time  $t_o$  must be known. Two methods for calculation of the horizontal deployment reference time are available. One is via equation (9) from page A-7 of Appendix A and the other via equation (10) from page 5-61 of Reference 2.

$$t_o = \frac{2W}{\rho g V_s C_D S_o} \left[ \epsilon \left[ \frac{\frac{g \rho V_o}{2W} \left[ \frac{C_D S_o}{A_{M_o} - A_{s_o} k \left( \frac{C.P. \rho}{2} \right)^{1/2}} \right]} \right] - 1 \right] \quad (9)$$

From Table 2, page A-15 of Appendix A, the following inflated shape data were obtained for a 30-gore solid cloth flat circular parachute. See Figure 24 of Appendix A for shape nomenclature. Steady-state inflated canopy radius:

$$\frac{2\bar{a}}{D_o} = 0.668; \frac{N}{a} = 0.827; \frac{b}{a} = 0.6214; \frac{b'}{a} = 0.7806$$

$$\bar{a} = \frac{0.668 \times 35}{2}$$

$$\bar{a} = 11.69 \text{ ft.}$$

Steady-state mouth area:

$$A_{M_0} = \pi \bar{a}^2 \left[ 1 - \left( \frac{N/\bar{a} - b/\bar{a}}{b'/\bar{a}} \right)^2 \right]$$

$$A_{M_0} = \pi (11.69)^2 \left[ 1 - \left( \frac{0.827 - 0.6214}{0.7806} \right)^2 \right]$$

$$A_{M_0} = 399.53 \text{ ft}^2$$

Steady-state canopy volume of air to be collected,  $V_0$  geometric.

$$V_0 = \frac{2}{3} \pi \bar{a}^3 \left[ \frac{b}{\bar{a}} + \frac{b'}{\bar{a}} \right]$$

$$V_0 = \frac{2}{3} \pi (11.69)^3 [0.6214 + 0.7807]$$

$$V_0 = 4690.83 \text{ ft}^3$$

The MIL-C-7020, type III canopy cloth airflow constant is  $k = 1.46$  and the average pressure coefficient is taken to be  $C.P. = 1.7$  then:

$$t_0 = \frac{14 \times 200}{0.0021753 \times 32.2 \times 340 \times 721.58} \left[ e^{K_1} - 1 \right]$$

$$K_1 = \frac{32.2 \times 0.0021753 \times 4690.33}{2 \times 200} \left[ \frac{721.58}{399.53 - 962.1(1.46) \left( \frac{0.0021753 \times 1.7}{2} \right)^{1/2}} \right]$$

$$t_0 = 0.773 \text{ sec.}$$

Knacke, Reference 2, presents the inflation time as

$$t_f = \frac{nD_0}{V_s}$$

$$t_f = \frac{8 \times 35}{340}$$

$$t_f = 0.824 \text{ sec.}$$

where  $n=8$  for solid cloth parachutes

While equation (10) is more convenient than (9) to use, equation (9) gives the effects of altitude, mass, and cloth rate of airflow; both values are estimates of the inflation time. Equation (9) was theoretically derived. Equation (10) was empirically developed by other experimenters from numerous field test data. The parachute system of Example 1 for standard air density at an altitude of 1000 feet yields values of  $t_0=0.839$  seconds and  $t_f=0.824$  seconds. The closeness of the theoretical  $t_0$  and the empirical  $t_f$  values indicates that the application of the criterion listed below is a reasonable approach to the inflation time calculation.

- a. Average pressure coefficient
- b. Cloth permeability
- c. The trajectory velocity is taken as the canopy inflow velocity
- d. The ratio of the instantaneous mouth area to the steady-state mouth area is equal to the instantaneous drag-area ratio
- e. The ratio of the instantaneous pressurized canopy area to the canopy surface area,  $S_0$ , is equal to the instantaneous drag-area ratio
- f. The volume of air to be collected during the inflation process is represented by  $V_0$ .

As a demonstration of the cloth rate of airflow effects in equation (9), replacement of the canopy cloth of example 1 with a high rate of airflow, three momme silk cloth ( $K=7.43$ ) yields an inflation reference time of  $t_0=99.76$  sec. under the example 1 operational conditions. This time exceeds the time of fall from 3,000 feet and the system would appear to an observer as a partial inflation. The same system deployed horizontally at 20,000 feet, at constant dynamic pressure, has an inflation reference time of  $t_0=1.5$  sec. When the area term

$$A_{m0} - A_{s0}k\left(\frac{C.P.\rho}{2}\right)^{1/2} = 0$$

equals zero, the inflation reference time is infinite, (eq. 9). As the area term approaches zero,  $t_0$  increases exponentially. It is possible for the inflation time to be extended to the point that the parachute system is not practical even though the area ratio is not zero. Parachute canopies without cloth airflow,  $K=0$ , always inflate.

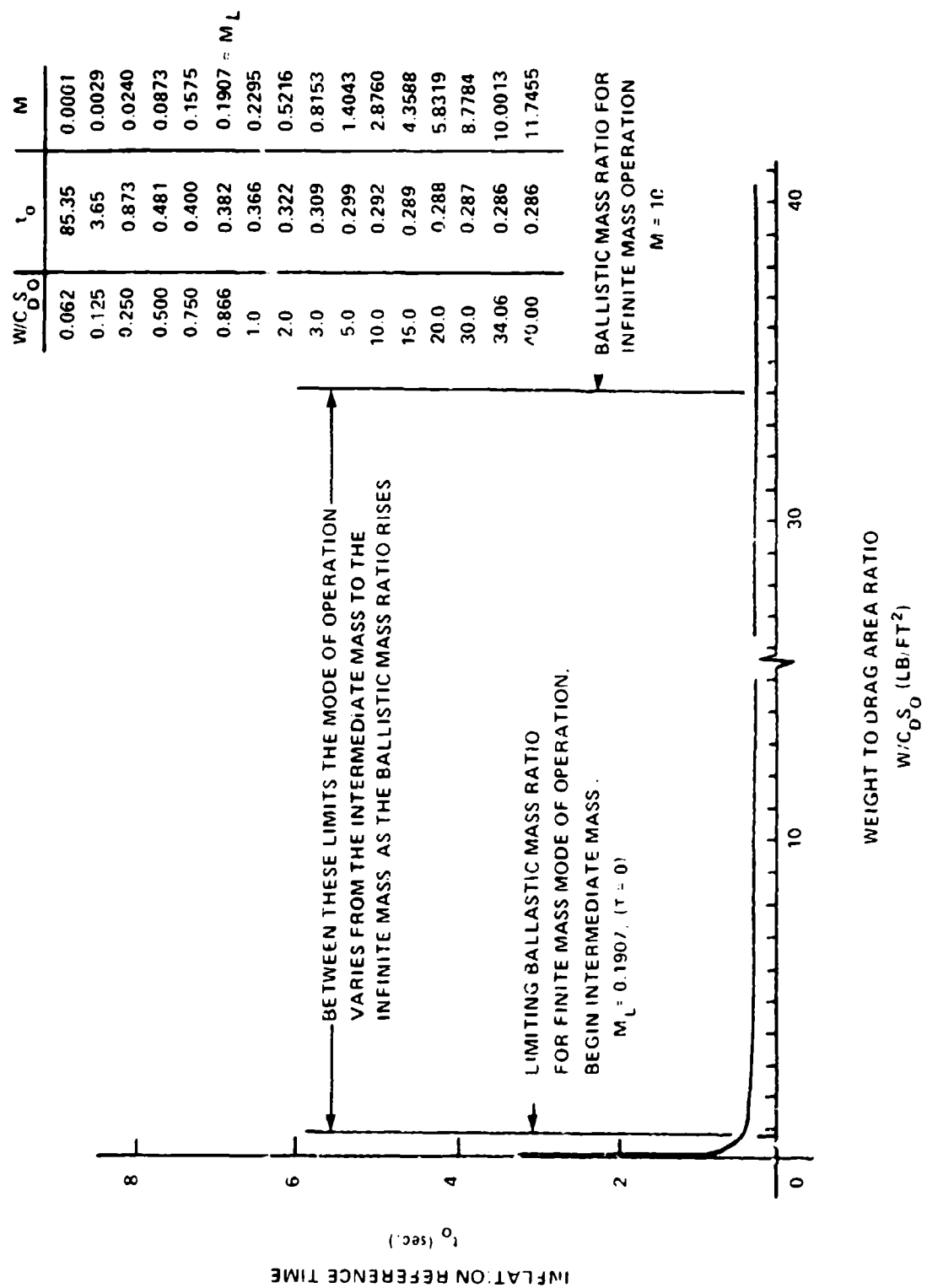


FIGURE 2. VARIATION OF THE INFLATION REFERENCE TIME AS A FUNCTION OF SYSTEM WEIGHT FOR THE FLAT CIRCULAR SOLID CLOTH PARACHUTE OF EXAMPLE ONE.

When using generalized expressions such as equation (10), it is important to know the mode of operation for which the formula was determined. The identical parachute used in finite mass, intermediate mass, or infinite mass systems experiences a variation in inflation time due to its mode of use. At the time  $t_0$  all inflations have collected the same volume of air. Finite mass inflations experience a significant velocity reduction during the inflation process which limits the rate of airflow into the canopy and extends the inflation time. Infinite mass deployments, on the other hand, can be nearly constant velocity which maintains a higher rate of mass flow into the canopy and decreases the inflation time. Actual constant velocity infinite mass operation produces the minimum inflation time. The inflation reference times, for the parachute of Example 1, are plotted in Figure 2 as a function of weight-to-drag-area ratio for equation (9). The finite mass and infinite mass limiting ballistic mass ratios for solid cloth parachutes are referenced on the graph.

The trends of Figure 2 show that the principal variation of the inflation reference time occurs in the finite mass mode of operation. By the transition from finite mass to low intermediate mass a near minimum inflation reference time is reached. This quickly converges to an essentially constant value for the high end of the intermediate mass and infinite mass regimes. Similar trends for other types of parachutes are a reasonable extension of the premise since it is based on variable rates of flow filling a constant volume.

Ballistic Mass Ratio for  $t_0 = 0.773$  sec.

$$M = \frac{2W}{\rho g V_s t_0 C_D S_0}$$

$$M = \frac{2 \times 200}{0.0021753 \times 32.2 \times 340 \times 0.773 \times 721.58}$$

$$M = 0.0301$$

Since the ballistic mass ratio is less than the limiting value of 0.1907, the inflation performance is in the finite mass range of operation and  $t_0 = t_f$ . The following formulae were obtained from Table 12 of Reference 1 for values of  $j=6$  and  $\tau = 0$ .

The time of occurrence of the maximum shock force during canopy inflation.

$$\frac{t}{t_0} \text{ at } X_{i \max} = \left( \frac{21M}{4} \right)^{1.7}$$

$$\frac{t}{t_0} \text{ at } X_{i \max} = \left( \frac{21 \times 0.0301}{4} \right)^{1.7}$$

$$\frac{t}{t_0} \text{ at } X_{i \max} = 0.7685$$

The maximum shock factor:

$$X_{i \max} = \frac{16}{49} \left( \frac{21M}{4} \right)^{6.7}$$

$$X_{i \max} = \frac{16}{49} \left( \frac{21 \times 0.0301}{4} \right)^{6.7}$$

$$X_{i \max} = 0.0672$$

Maximum shock force in the horizontal mode of deployment.

$$F_{\max} = X_{i \max} F_s$$

$$F_{\max} = 0.0672 \times 90,726.7$$

$$F_{\max} = 61 \text{ ,}$$

The magnitude of the opening shock force varies with the inflation reference time of the parachute in the finite mass regime of operation. In the field there is often a variation in the measured inflation time from the nominal calculated value, which results in a variation in opening shock force. A survey of horizontal opening shock forces was made via the foregoing technique for assigned values of  $t_0$  from 0.5 through 1.0. The results are plotted in Figure 3 for the horizontal deployment mode forces and the "lg added" rule of thumb. The particular values of  $t_0$  and  $t_f$  for example (1) mark the range of the nominal expected performance.

A method of calculating "t<sub>0</sub>" in the vertical mode of deployment is required so that the horizontal and vertical inflation reference times can be compared for identical systems deployed at the same altitude and velocity.

The inflation reference time "t<sub>0</sub>" in the vertical deployment mode can be determined from the basic mass flow equation used to calculate the horizontal deployment "t<sub>0</sub>". Following the method of Section IV of Appendix A for solid cloth parachutes.

$$d_m = m_{inflow} - m_{outflow}$$

$$\rho \frac{dV}{dt} = \rho VA_m - \rho A_s P$$

Instantaneous canopy mouth area.

$$A_m = A_{m0} \left( \frac{t}{t_0} \right)^6 \quad \text{FOR } \tau = 0$$

Instantaneous pressurized canopy cloth area.

$$A_s = A_{s0} \left( \frac{t}{t_0} \right)^6 \quad \text{FOR } \tau = 0$$

Instantaneous cloth rate of airflow.

$$P = k \left( \frac{C.P.\rho}{2} \right)^n V^{2n} \quad \text{C.F.S./FT}^2$$

Where the instantaneous velocity is determined by equation (4) for  $\tau = 0$ .

$$V = \int_{V=V_s}^V dv = \int_{t=0}^t \left( g - \frac{V^2}{MV_s t_0} \left( \frac{t}{t_0} \right)^6 \right) dt \quad (4)$$

The calculated canopy volume,  $V_o$  calc, is determined from equation (11).

$$V_{o\text{calc}} = \int_{V=0}^{V_o} dV = \int_{t=0}^{t_o} \left[ VA_{mo} \left( \frac{t}{t_o} \right)^6 - A_{so} \left( \frac{t}{t_o} \right)^6 k \left( \frac{C.P.\rho}{2} \right)^n v^{2m} \right] dt \quad (11)$$

A program for calculating  $t_o$  for solid cloth parachutes and the opening shock force profile during the inflation of several parachute types is provided in Table 1. Equations (4), (11), and (12) are programmed together with the vertical deployment opening shock equations (2) through (8) in FORTRAN IV language. The included examples were calculated via the program using a VAX 780 computer. The program operates in two modes. Mode 1, for solid cloth parachutes, calculates the vertical deployment reference time  $t_o$  for the parachute system parameters and operational deployment data, and then calculates the opening shock profile during inflation. A typical data print out is shown in Table 2. It is necessary to estimate an initial value of " $t_o$ ". The program calculates the canopy volume for the estimated time and compares the  $V_o$  calc to the volume derived from the canopy geometry. If the calculated volume is not within specified limits, the program adjusts " $t_o$ " by equation (12) and reiterates the program until the calculated volume is within the specified limits.

$$t_o = t_o \left( \frac{V_o \text{ geometric}}{V_o \text{ calc.}} \right) \quad (12)$$

Mode 2 of the program calculates opening shock profiles for input values of  $t_o$ . Mode 2 analysis of other types of parachutes is possible by the selection of the proper values of "j" (1/2, 1, 2, 3, 4, 5, or 6) and "r". The opening shock force variation for examples (1) and (2) are plotted in Figures 3 and 4. The nominal  $t_o$  for  $n=0.632$  was calculated by the program in mode 1 and the force-time survey was calculated in mode 2.

Figure 3 illustrates that parachutes deployed in a vertical toward-the-earth trajectory inflate faster than the same system deployed horizontally at the same altitude and velocity.

Inflation reference times for parachute types other than solid cloth canopies can be developed from the mass flow equation. This requires that the flow through the canopy be expressed in a form similar to the solid cloth canopy cloth permeability,  $P$ , where the rate of flow per unit area is a function of the pressure differential across the cloth or grid.

**TABLE 1. INSTANTANEOUS DRAG AREA, VELOCITY, OPENING SHOCK FORCE, AND DISTANCE OF FALL OF A PARACHUTE DEPLOYED IN VERTICAL FALL.**

THIS PROGRAM CALCULATES THE INSTANTANEOUS DRAG AREA, VELOCITY, OPENING SHOCK FORCE, AND DISTANCE OF FALL OF A PARACHUTE DEPLOYED IN VERTICAL FALL.

THE PROGRAM OPERATES IN TWO MODES:

- MODE 1 - CALCULATES THE INFLATION TIME AND PERFORMANCE PROFILES FOR SOLID CLOTH PARACHUTES (TO INPUT AS INITIAL ESTIMATE) (IOPT = 1)
- MODE 2 - CALCULATES THE PERFORMANCE PROFILES FOR VARIOUS TYPES OF PARACHUTES (J). INFLATION TIME INPUT IS REQUIRED (IOPT = 2)

INPUT. IOPT - 1 (FOR MODE 1)  
          - 2 (FOR MODE 2)

INPUT NEEDED FOR BOTH MODES:

RHO - AIR DENSITY AT GIVEN ALTITUDE (SLUGS/FT<sup>3</sup>)  
 VS - VELOCITY AT SUSPENSION LINE STRETCH (FT/SEC)  
 CDSO - DESIGN DRAG AREA (FT<sup>2</sup>)  
 TO - IOPT=1 INITIAL GUESS FOR INFLATION REF. TIME (SEC)  
       IOPT=2 ACTUAL INFLATION REFERENCE TIME (SEC)  
 W - WEIGHT (LBS)  
 J - =6 FOR FLAT CIRCULAR PARACHUTE  
       =1 FOR RIBBON TYPE OF PARACHUTE

INPUT NEEDED FOR IOPT = 1 ONLY.

AMO - STEADY-STATE MOUTH AREA (FT<sup>2</sup>)  
 ASO - CANOPY DESIGN SURFACE AREA (FT<sup>2</sup>)  
 K - CLOTH PERMEABILITY CONSTANT  
 CP - PRESSURE COEFFICIENT  
 N - CLOTH PERMEABILITY EXPONENT  
 VO - GEOMETRIC VOLUME (FT<sup>3</sup>)

```

REAL*4 N
TODEN=100000
5 PRINT *, 'INPUT IOPT'
READ(5, *, END=100) IOPT
PRINT *, 'INPUT RHO, VS, CDSO, TO, W, J'
READ(5, *)RHO, VS, CDSO, TO, W, J
IF(IOPT.EQ.2) GO TO 3
PRINT *, 'INPUT AMO, ASO, XK, CP, N, VO'
READ(5, *)AMO, ASO, XK, CP, N, VO
3 DT=TO/TODEN
TAU=0
G=32.2
S=0.
X=TAU
CDS=CDSO
FS=.5*RHO*VS**2*CDSO
F=TAU*FS
VOL=0
IPASS=0

```

TABLE 1. (CONT.)

```

DT=10.*DT
IF (IOPT.EQ.2) GO TO 8
7 V=VS
VOL=0.
T=0.
XM=(2.*W)/(RHO*G*CDSO*VS*TO)
6 DV=(G-V**2/(XM*VS*TO))*(T/TO)**J)*DT
DVOL=(V*AMO*(T/TO)**J-ASO*(T/TO)**J*XK*(CP*RHO/2.))**N
1 *V**(2.*N))*DT
VOL=VOL+DVOL
V=V+DV
T=T+DT
IF (T.GE.TO) GO TO 4
GO TO 6
4 IF (VOL.GT.(VO-10.) .AND. VOL.LT.(VO+10.)) GO TO 8
TO=TO*(VO/VOL)
IF (IPASS.GT.50) STOP
IPASS=IPASS+1
GO TO 7
8 CONTINUE
T=0.
V=VS
DT=DT/10.
WRITE(6,10) RHO,VS,CDSO,W,TO, XM, J, FS
10 FORMAT(1H1, 'DENSITY='1PE12.5,2X, 'V(S)='OPFB.1,2X, 'CDSO='FB.2,
1 2X, 'W='F7.1,2X, 'T(0)='F6.3,2X, 'M='1PE12.5,2X, 'J='I2,2X,
2 'FS='1PE12.5)
IF (IOPT.EQ.1) WRITE(6,11) AMO,ASO,XK,CP,N,VO,VOL
11 FORMAT(1H0,4X, 'AM='',OPFB.2,7X, 'ASO='',OPFB.2,5X, 'K='',OPFB.3,1X,
4 'CP='',OPFB.3,5X, 'N='',OPFB.3,1X, 'VO='',1PE12.5,7X, 'VOL='1PE12.5)
WRITE(6,20)
20 FORMAT(1H0,2X, 'TIME'2., 'TIME RATIO',2X, 'VEL RATIO',2X, 'DRAG AREA
1RATIO',2X, 'SHOCK FACTOR',3X, 'SHOCK FORCE',2X, 'DIST. OF FALL')
30 FORMAT(1X,F6.2,2F12.5,F17.7,1P2E14.5,OPF15.2)
LCOUNT=5
35 IF (T/TO.GT.1.51) GO TO 5
IF (LCOUNT.LT.54) GO TO 38
WRITE(6,37)
37 FORMAT(1H1)
WRITE(6,20)
LCOUNT=3
38 LCOUNT=LCOUNT+1
WRITE(6,30) T, T/TO, V/VS, CDS/CDSO, X, F, S
TOLD=T+.02
IF (DT.GT.0.02) TOLD=T+DT
40 T=T+DT
IF (T.GT.TOLD) T=TOLD
TGVTO=(1-TAU)*(T/TO)**J + TAU
CDS=CDSO*TGVTO
DV=(G-V**2*TGVTO/(XM*VS*TO))*DT
DS=V*DV/(G-V**2*TGVTO/(XM*VS*TO))
V=V+DV
S=S+DS
X=(V/VS)**2*CDS/CDSO
F=X*FS
IF (T.LT.TOLD) GO TO 40
GO TO 35
100 STOP
END

```

TABLE 2. SUMMARY OF THE FLAT CIRCULAR SOLID CLOTH PARACHUTE VERTICAL TRAJECTORY CALCULATIONS FOR A VALUE OF TIME INCREMENT  $\Delta t = 1/100,000$

DEPLOYMENT CONDITIONS		SYSTEM PARAMETERS						
ALTITUDE = 3,000 FT		STEADY STATE DRAG AREA, $C_D S_0 = 721.58 \text{ FT}^2$						
DENSITY = 0.0021753 SLUGS/FT <sup>3</sup>		WEIGHT, $W = 200 \text{ LB}$						
VELOCITY, $V_s = 340.0 \text{ f.p.s.}$		INFLATION TIME, $t_0 = 0.907 \text{ SECONDS}$						
$D_0 = 35 \text{ FT}$		STEADY STATE DRAG FORCE, $F_s = 90725.9 \text{ LB}$						
$j = 6.0$		$M = 0.02567$						
$\tau = 0$		$n = 0.632$						
TIME SEC	TIME RATIO	VELOCITY RATIO	DRAG AREA RATIO	SHOCK FACTOR	SHOCK FORCE (LB)	DISTANCE OF FALL (FT)		
0 00	0 00000	1 00000	0 0000000	0 00000E+00	0 00000E+00	0 00		
0 02	0 02206	1 00198	0 0000000	1 15778E-10	1 05044E-05	6 81		
0 04	0 04412	1 00395	0 0000000	7 43904E-09	6 74932E-04	13 63		
0 06	0 06619	1 00593	0 0000001	8 50692E-08	7 71819E-03	20 47		
0 08	0 08825	1 00790	0 0000005	4 79853E-07	4 35364E-02	27 32		
0 10	0 11031	1 00988	0 0000018	1 83768E-06	1 66730E-01	34 19		
0 12	0 13237	1 01185	0 0000054	5 50877E-06	4 99802E-01	41 06		
0 14	0 15444	1 01378	0 0000136	1 39439E-05	1 26511E+00	47 95		
0 16	0 17650	1 01577	0 0000302	3 11798E-05	2 82889E+00	54 86		
0 18	0 19856	1 01737	0 0000613	6 34341E-05	5 75527E+00	61 77		
0 20	0 22062	1 01916	0 0001153	1 19784E-04	1 08678E+01	68 70		
0 22	0 24269	1 02046	0 0002043	2 12954E-04	1 93209E+01	75 54		
0 24	0 26475	1 02259	0 0003443	3 60080E-04	3 76695E+01	82 57		
0 26	0 28681	1 02408	0 0005566	5 83772E-04	5 29648E+01	89 55		
0 28	0 30887	1 02534	0 0008683	9 12890E-04	8 28251E+01	96 51		
0 30	0 33094	1 02626	0 0013136	1 36349E-03	1 25521E+02	103 48		
0 32	0 35300	1 02670	0 0019348	2 03948E-03	1 85039E+02	110 45		
0 34	0 37506	1 02648	0 0027836	2 93297E-03	2 65103E+02	117 43		
0 36	0 39712	1 02536	0 0039224	4 13385E-03	3 74151E+02	124 39		
0 38	0 41918	1 02508	0 0054254	5 67873E-03	5 15222E+02	131 35		
0 40	0 44125	1 01977	0 0073806	7 66785E-03	6 95692E+02	138 29		
0 42	0 46331	1 01050	0 0098707	1 01506E-02	9 21055E+02	145 20		
0 44	0 48537	1 00545	0 0130750	1 32181E-02	1 19226E+03	152 06		
0 46	0 50743	0 99447	0 0170718	1 68834E-02	1 53180E+03	158 85		
0 48	0 52950	0 98007	0 0220284	2 11685E-02	1 92040E+03	165 56		

TABLE 2. (CONT.)

TIME SEC	TIME RATIO	VELOCITY RATIO	DRAG AREA RATIO	SHOCK FACTOR	SHOCK FORCE (LB)	DISTANCE OF FALL (FT)
0 50	0 55156	0 96174	0 0281549	2 60413E-02	2 36269E+03	172 16
0 52	0 57362	0 93400	0 0356248	3 14109E-02	2 84987E+03	178 62
0 54	0 59568	0 91149	0 0446781	3 71192E-02	3 36777E+03	184 90
0 55	0 61775	0 87902	0 0555725	4 79392E-02	3 89581E+03	190 99
0 58	0 63981	0 84160	0 0685962	4 85853E-02	4 40811E+03	196 84
0 60	0 66187	0 79952	0 0840696	5 37401E-02	4 87575E+03	202 41
0 62	0 68393	0 75334	0 1013486	5 80857E-02	5 27002E+03	207 59
0 64	0 70600	0 70388	0 1238259	5 13498E-02	5 56617E+03	212 64
0 66	0 72805	0 65216	0 1489344	5 33430E-02	5 74702E+03	217 25
0 68	0 75012	0 59930	0 1781496	5 39840E-02	5 80517E+03	221 50
0 70	0 77218	0 54647	0 2119920	5 33063E-02	5 74368E+03	225 39
0 72	0 79424	0 49473	0 2510304	6 14423E-02	5 57457E+03	228 93
0 74	0 81631	0 44503	0 2958840	5 86016E-02	5 31683E+03	232 12
0 75	0 83837	0 39611	0 3472264	5 50316E-02	4 99294E+03	234 98
0 78	0 86043	0 35447	0 4057877	5 09856E-02	4 62585E+03	237 53
0 80	0 88249	0 31442	0 4723577	4 6697E-02	4 23672E+03	239 80
0 82	0 90456	0 27808	0 5477901	4 23613E-02	3 84338E+03	241 91
0 84	0 92662	0 24544	0 6330046	3 81320E-02	3 45965E+03	243 59
0 86	0 94868	0 21634	0 7289903	3 41174E-02	3 09542E+03	245 16
0 88	0 97074	0 19056	0 8368103	3 03874E-02	2 75700E+03	246 54
0 90	0 99281	0 16785	0 9576039	2 69798E-02	2 44784E+03	247 75
0 92	1 01487	0 14792	1 0925910	2 39078E-02	2 16912E+03	248 82
0 94	1 03693	0 13049	1 2430770	2 11673E-02	1 92048E+03	249 77
0 96	1 05899	0 11527	1 4104518	1 87425E-02	1 70048E+03	250 60

W = 200 LB  
 V<sub>s</sub> = 340 f.p.s.  
 Alt. = 3,000 FT  
 τ = 0

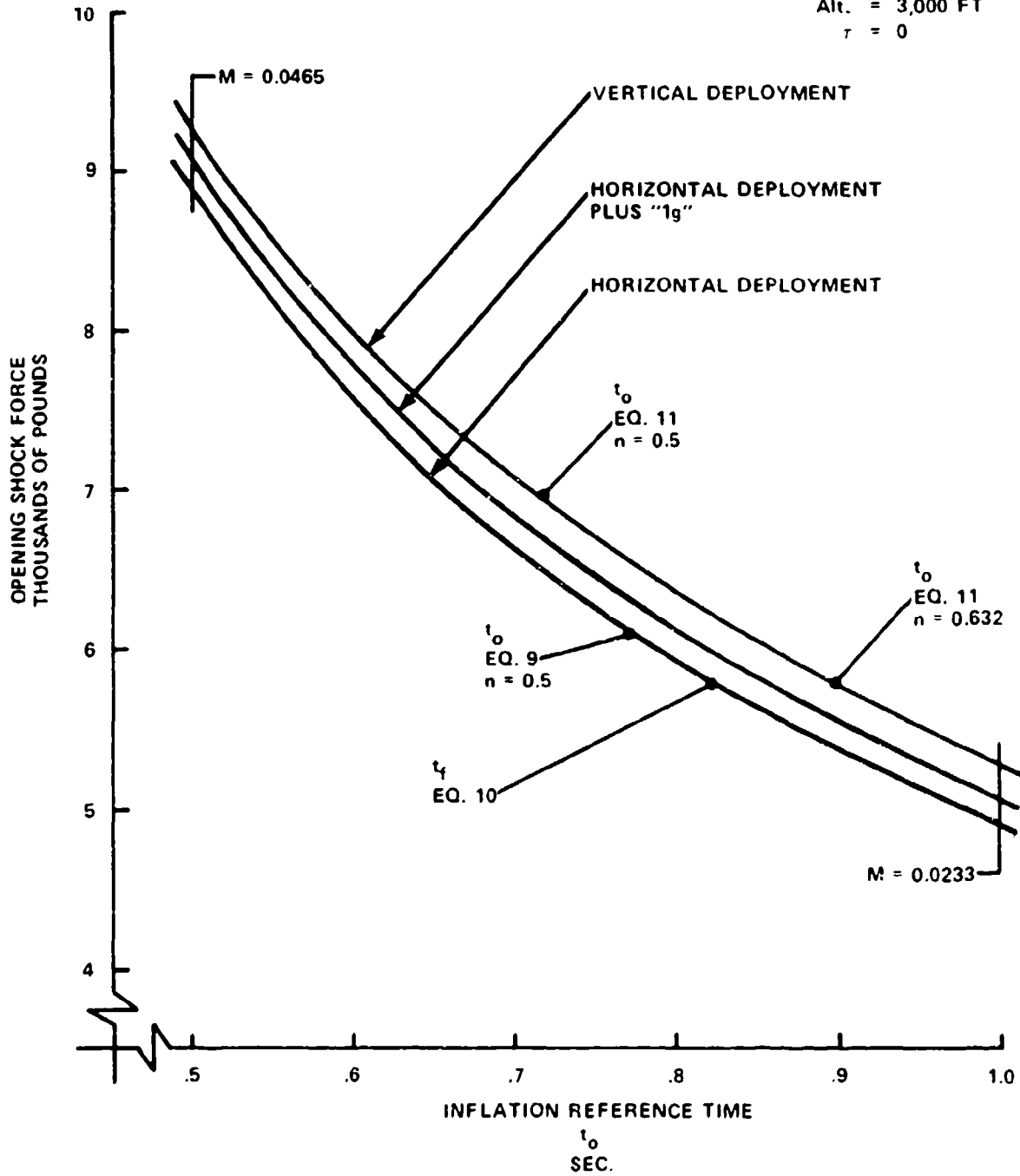


FIGURE 3. OPENING SHOCK FORCE IN THE HORIZONTAL AND VERTICAL DEPLOYMENT MODES AS A FUNCTION OF INFLATION REFERENCE TIME FOR SYSTEM WEIGHT OF 200 POUNDS

The various  $t_0$  and  $t_f$  times noted on the graph are the particular solutions for the deployment conditions of example 1. All of the ballistic mass ratios,  $M$ , in the calculations are less than the limiting value ( $M_L=0.1907$ ) for finite mass operation. Also, the calculated opening shock forces are less than the suspension line constructed strength ( $F_C=16,500$  lb) which indicates a practical system for the opening shock requirement. Examination of the inflation times for equations (9) and (11) for  $n=0.5$  demonstrates that the vertical deployment parachute inflation time is reduced even though the system parameters of deployment altitude and velocity were identical. The reason for this is that parachutes are energy dissipators. In the horizontal deployment mode the additional added potential energy of the system weight falling a short distance during inflation is not included in the calculations. In the vertical mode considerably more potential energy is absorbed into the system resulting in less trajectory velocity reduction during inflation and hence a shorter inflation reference time.

In field tests the inflation reference time often varies from the calculated value. One cause of this is the variation of airflow through the cloth as it is manufactured and/or handled. The cloth airflow constants ( $k, n$ ) would have to be true average values for each parachute which requires so many fabric tests as to be unreasonable. The effects of varying  $n$  for a constant  $k$  are shown in Figure 3 for equation (11). As  $n$  increases from 0.5 the rate of cloth airflow is augmented, extending the inflation reference time and reducing the opening shock force.

For any constant inflation reference time, the vertical deployment mode opening shock force exceeds the "rule of thumb" value.

Example 2: Investigate the feasibility of retarding a 2000-lb. payload using the parachute system of example 1.

Figure 4 presents a horizontal deployment analysis using the methods of example 1 for assigned values of  $t_0$  from 0.3 to 0.8 seconds. The vertical deployment analysis, using the program modes of Table 1 was conducted using the same  $t_0$  range. The particular inflation reference times for the conditions of example 2 was computed by equation (9) and equation (11). The increased system weight caused a reduction in all values of  $t_0$  as expected from Figure 2. The inflation time calculated from equation (10) is unchanged from Figure 3 since equation 10 does not adjust for weight variation.

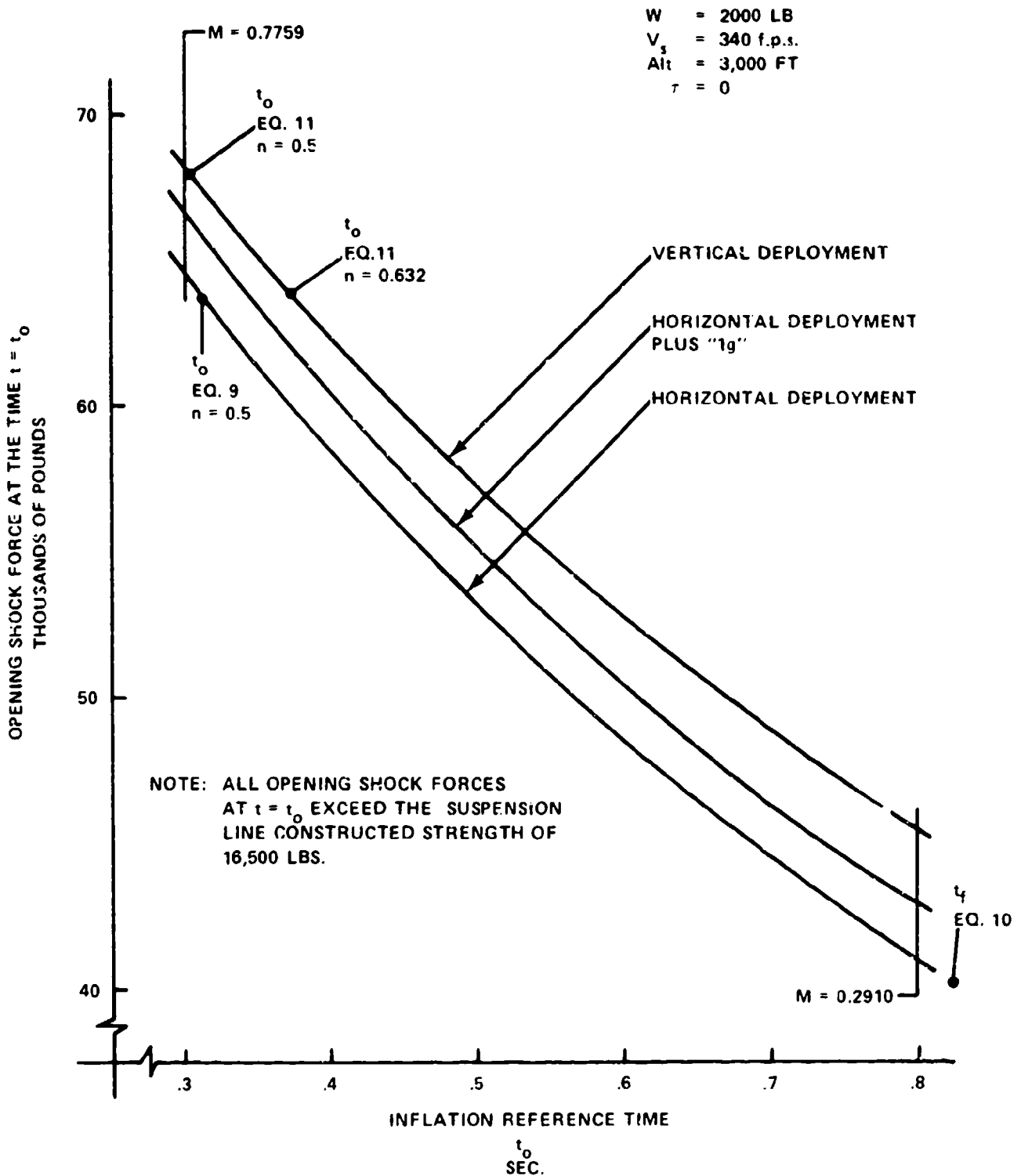


FIGURE 4. OPENING SHOCK FORCES AT THE INFLATION REFERENCE TIME  $t = t_0$  IN THE HORIZONTAL AND VERTICAL DEPLOYMENT MODES AS A FUNCTION OF INFLATION REFERENCE TIME FOR A SYSTEM WEIGHT OF 2000 POUNDS

The analysis ballistic mass ratios exceed the finite mass limiting value ( $M_L=.1907$ ). This indicates that the maximum opening shock force occurs during the over inflation phase of deployment. Calculation of the opening shock force at  $t=t_0$  produces shock magnitudes in excess of the suspension line constructed strength resulting in system failure prior to reaching the calculated  $t_0$ . The parachute of example 1 is not a practical application for the heavier weight of example 2.

## SUMMARY AND CONCLUSIONS

A method of calculating the opening shock force of vertically deployed, toward-the-earth parachutes has been developed. The analysis utilizes a dynamic drag-area signature of the form  $C_D S / C_D S_0 = (1-\tau) (t/t_0)^2 + \tau$  and is applicable to several types of parachutes. Unlike the closed form analysis of Reference 1, a furnished computer program is required for solution. The program has two modes of operation. Mode 1 is for the solid cloth canopy family of parachutes. The particular inflation reference time for the system and deployment condition is computed, and this value is used to calculate the instantaneous drag area, velocity, force profile, and distance of fall during the inflation process. Mode 2 requires inflation reference time as input data, and is used for all types of parachutes. This mode is convenient for conducting surveys to evaluate expected opening shock force variation as a function of inflation time. Vertical opening shock forces calculated by this technique exceed the rule of thumb. A time step of  $dt=t_0/100000$  in the program gives acceptable results.

The inflation reference time of a parachute system in vertical fall is less than the inflation time of the same system deployed horizontally at the identical altitude and velocity.

The inflation reference time of a given parachute system, for constant launch conditions, depends upon the system weight. For low weight finite mass assemblies the inflation reference time is extended due to the trajectory velocity reduction during inflation. The inflation reference time reduces rapidly as the system weight increases. After the finite mass to intermediate mass transition most of the inflation reference time decrease has been realized. As the system approaches the infinite mass condition the inflation reference time approaches a constant value.

Parachutes of light construction, such as personnel designs, depend upon the reduction of trajectory velocity during inflation for successful operation. As the system weight is increased the velocity reduction is not realized and the opening shock forces will eventually exceed the parachute constructed strength, resulting in failure.

A closed form inflation reference time equation for horizontal deployment is presented. This equation demonstrates that the inflation distance ( $V_{gt_0}$ ) is a function of altitude, canopy cloth permeability, and system mass and area ratios. The particular inflation reference time solution for example (1) is in close agreement with the empirical approach. While more complicated, the theory accounts for more variables and is worthwhile as in the example of the use of the three momme silk

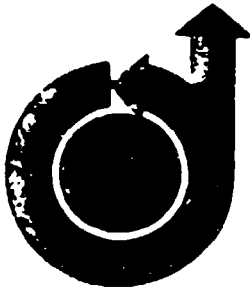
cloth at sea level and 20,000 feet. Usually, the inflation distance is considered only as a velocity-time effect. The closeness of the theoretical and empirical inflation time values at low altitudes indicates that the method of application of the following parameters, in the filling time calculation, are reasonable:

- a) Use of the trajectory velocity as the canopy inflow velocity
- b) Use of the cloth permeability,  $P$ , to determine instantaneous cloth airflow rates
- c) Correlation of the instantaneous mouth inflow area, and instantaneous pressurized canopy surface area with the drag area ratio variation
- d) Canopy volume of air,  $V_0$ , which is to be collected in the inflation process.

As the cloth rate of airflow exponent "n" increases from 0.5, the rate of cloth airflow increases and the canopy inflation time is extended.

REFERENCES

1. Ludtke, W.P., "Notes On A Generic Parachute Opening Force Analysis." NSWC TR 86-142.
2. Knacke, T., "Notes from the Helmut G. Heinrich Short Course on Decelerator Systems." lecture at the Sandia National Laboratories, Albuquerque, N.M, July 1985.



NSWC TR 87-96

Appendix A

**AIAA Paper  
No. 73-477**

**A TECHNIQUE FOR THE CALCULATION OF THE  
OPENING-SHOCK FORCES FOR SEVERAL TYPES OF  
SOLID CLOTH PARACHUTES**

by  
**W. P. LUDTKE**  
Naval Ordnance Laboratory  
Silver Spring, Maryland

# **AIAA 4th Aerodynamic Deceleration Systems Conference**

**PALM SPRINGS, CALIFORNIA / MAY 21-23, 1973**

First publication rights reserved by American Institute of Aeronautics and Astronautics,  
1290 Avenue of the Americas, New York, N. Y. 10019. Abstracts may be published without  
permission if credit is given to author and to AIAA. (Price: AIAA Member \$1.50, Nonmember \$2.00)

Note: This paper available at AIAA New York office for six months,  
thereafter, photoprint copies are available at photocopy prices from  
AIAA Library, 750 3rd Avenue, New York, New York 10017

TECHNIQUE FOR THE CALCULATION OF THE OPENING-SHOCK FORCES FOR  
SEVERAL TYPES OF SOLID CLOTH PARACHUTES

W. P. Ludtke  
Naval Ordnance Laboratory  
Silver Spring, Maryland

Abstract

An analytical method of calculating parachute opening-shock forces based upon wind-tunnel derived drag area time signatures of several solid cloth parachute types in conjunction with a scale factor and retardation system steady-state parameters has been developed. Methods of analyzing the inflation time, geometry, cloth airflow properties and materials elasticity are included. The effects of mass ratio and altitude on the magnitude and time of occurrence of the maximum opening shock are consistent with observed field test phenomena.

I. Introduction

In 1965, the Naval Ordnance Laboratory (NOL) was engaged in a project which utilized a 35-foot-diameter, 10-percent extended-skirt parachute (type T-10) as the second stage of a retardation system for a 250-pound payload. Deployment of the T-10 parachute was to be accomplished at an altitude of 100,000 feet. In this rarefied atmosphere, the problem was to determine the second stage deployment conditions for successful operation. A search of available field test information indicated a lack of data on the use of solid cloth parachutes at altitudes above 30,000 feet.

The approach to this problem was as follows: Utilizing existing wind-tunnel data, low-altitude field test data, and reasonable assumptions, a unique engineering approach to the inflation time and opening-shock problem was evolved that provided satisfactory results. Basically, the method combines a wind-tunnel derived drag area ratio signature as a function of deployment time with a scale factor and Newton's second law of motion to analyze the velocity and force profiles during deployment. The parachute deployment sequence is divided into two phases. The first phase, called "unfolding phase," where the canopy is undergoing changes in shape, is considered to be inelastic as the parachute inflates initially to its steady-state aerodynamic size for the first time. At this point, the "elastic phase" is entered where it is considered that the elasticity of the parachute materials enters the problem and resists the applied forces until the canopy has reached full inflation.

The developed equations are in agreement with the observed performance of solid cloth parachutes in the field, such as the decrease of inflation time as

altitude increases, effects of altitude on opening-shock force, finite and infinite mass operation, and inflation distance.

II. Development of Velocity Ratio and Force Ratio Equations During the Unfolding Phase of Parachute Deployment

The parachute deployment would take place in a horizontal attitude in accordance with Newton's second law of motion.

$$\Sigma F = ma$$

$$-\frac{1}{2} \rho v^2 C_D S = \frac{W}{g} \frac{dv}{dt}$$

It was recognized that other factors, such as included air mass, apparent mass, and their derivatives, also contribute forces acting on the system. Since definition of these parameters was difficult, the analysis was conducted in the simplified form shown above. Comparison of calculated results and test results indicated that the omitted terms have a small effect.

$$\int_0^t C_D S dt = \frac{-2W}{\rho g} \int_{v_s}^v \frac{dv}{v^2} \quad (1)$$

Multiplying the right-hand side of equation (1) by

$$1 = \frac{v_s t_0 C_D S_0}{v_s t_0 C_D S_0}$$

and rearranging

$$\frac{1}{t_0} \int_0^t \frac{C_D S}{C_D S_0} dt = \frac{-2W}{\rho g v_s t_0 C_D S_0} v_s \int_{v_s}^v \frac{dv}{v^2} \quad (2)$$

In order to integrate the left-hand term of equation (2), the drag area ratio must be defined for the type of parachute under

analysis as a function of deployment reference time,  $t_0$ .

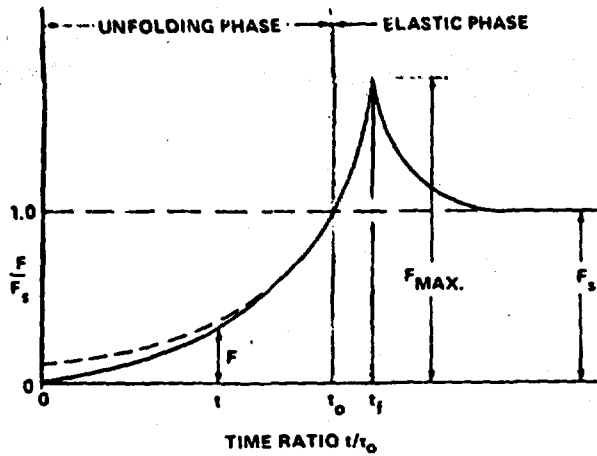


FIG. 1 TYPICAL INFINITE MASS FORCE-TIME HISTORY OF A SOLID CLOTH PARACHUTE IN A WIND TUNNEL

Figure 1 illustrates a typical solid cloth parachute wind-tunnel infinite mass force-time history after snatch. In infinite mass deployment, the maximum size and maximum shock force occur at the time of full inflation,  $t_f$ . However,  $t_f$  is inappropriate for analysis since it is dependent upon the applied load, structural strength, and materials elasticity. The reference time,  $t_0$ , where the parachute has attained its steady-state aerodynamic size for the first time, is used as the basis for performance calculations.

At any instant during the unfolding phase, the force ratio  $F/F_s$  can be determined as a function of the time ratio,  $t/t_0$ .

$$F = \frac{1}{2} \rho v^2 C_D S$$

$$F_s = \frac{1}{2} \rho v_s^2 C_D S_0$$

Since the wind-tunnel velocity and density are constant during infinite mass deployment

$$\frac{F}{F_s} = \frac{C_D S}{C_D S_0}$$

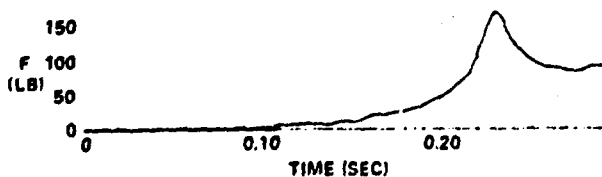


FIG. 2 TYPICAL FORCE-TIME CURVE FOR A SOLID FLAT PARACHUTE UNDER INFINITE MASS CONDITIONS.

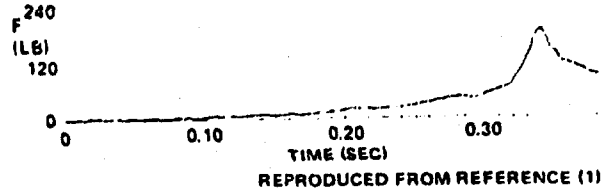


FIG. 3 TYPICAL FORCE-TIME CURVE FOR A 10% EXTENDED SKIRT PARACHUTE UNDER INFINITE MASS CONDITIONS.

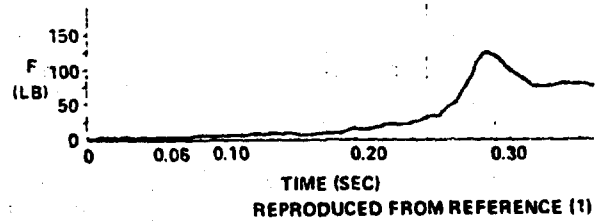


FIG. 4 TYPICAL FORCE-TIME CURVE FOR A PERSONNEL GUIDE SURFACE PARACHUTE UNDER INFINITE MASS CONDITIONS

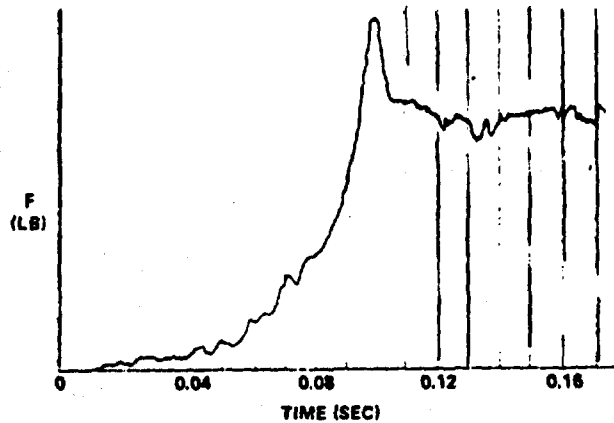


FIG. 5 TYPICAL FORCE-TIME SIGNATURE FOR THE ELLIPTICAL PARACHUTE UNDER INFINITE MASS CONDITIONS

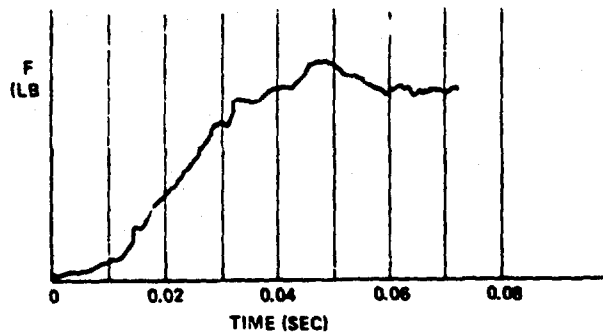


FIG. 6 TYPICAL FORCE-TIME SIGNATURE FOR THE RING SLOT PARACHUTE 20% GEOMETRIC POROSITY UNDER INFINITE MASS CONDITIONS

Infinite mass opening-shock signatures of several types of parachutes are presented in Figures 2 through 6. Analysis of these signatures using the force ratio,  $F/F_s$ , - time ratio,  $t/t_0$ , technique indicated a similarity in the performance of the various solid cloth types of

parachutes which were examined. The geometrically porous ring slot parachute displayed a completely different signature, as was expected. These data are illustrated in Figure 7. If an initial boundary

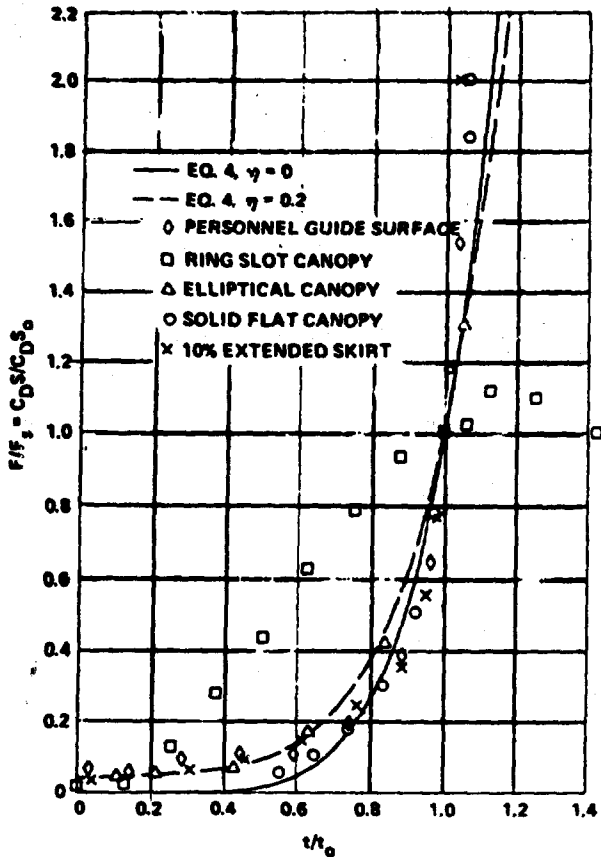


FIG. 7 DRAG AREA RATIO VS. TIME RATIO

condition of  $C_D S / C_D S_0 = 0$  at time  $t/t_0 = 0$  is assumed, then, the data can be approximated by fitting a curve of the form

$$\frac{C_D S}{C_D S_0} = \left(\frac{t}{t_0}\right)^6 \quad (3)$$

A more realistic drag area ratio expression was determined which includes the effect of initial area at line stretch.

$$\frac{C_D S}{C_D S_0} = \left[ \left(1 - \eta\right) \left(\frac{t}{t_0}\right)^2 + \eta \right]^2 \quad (4)$$

where  $\eta$  is the ratio of the projected mouth area at line stretch to the steady-state projected frontal area. Expanding equation (4)

$$\frac{C_D S}{C_D S_0} = \left(1 - \eta\right)^2 \left(\frac{t}{t_0}\right)^6 + 2\eta \left(1 - \eta\right) \left(\frac{t}{t_0}\right)^2 + \eta^2 \quad (5)$$

At the time that equation (5) was ascertained, it suggested that the geometry of the deploying parachute was independent of density and velocity. It was also postulated that although this expression had been determined for the infinite mass condition, it would also be true for the finite mass case. This phenomenon has since been independently observed and confirmed by Berndt and De Weese in reference (2).

Since the drag area ratio was determined from actual parachute deployments, it was assumed that the effects of apparent mass and included mass on the deployment force history were accommodated.

The right-hand term of equation (2) contains the expression

$$\frac{2W}{\rho g V_s t_0 C_D S_0} = M \quad (6)$$

This term can be visualized as shown in Figure 8 to be a ratio of the retarded mass (including the parachute) to an associated mass of atmosphere contained in a right circular cylinder which is generated by moving an inflated parachute of area  $C_D S_0$  for a distance equal to the product of  $V_s t_0$  through an atmosphere of density,  $\rho$ .

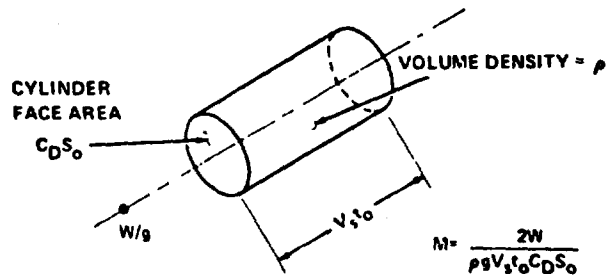


FIG. 8 VISUALIZATION OF THE MASS RATIO CONCEPT

The mass ratio,  $M$ , is the scale factor which controls the velocity and force profiles during parachute deployment. Substituting  $M$  and  $C_D S / C_D S_0$  into equation (2), integrating, and solving for  $V/V_s$

$$\frac{V}{V_s} = \frac{1}{1 + \frac{1}{M} \left[ \frac{(1 - \eta)^2}{7} \left(\frac{t}{t_0}\right)^7 + \frac{\eta(1 - \eta)}{2} \left(\frac{t}{t_0}\right)^3 + \eta^2 \frac{t}{t_0} \right]} \quad (7)$$

The instantaneous shock factor is defined as

$$x_1 = \frac{F}{F_s} = \frac{\frac{1}{2} \rho v^2 C_D S}{\frac{1}{2} \rho v_s^2 C_D S_0}$$

If the altitude variation during deployment is small, then, the density may be considered as constant

$$x_1 = \frac{C_D S}{C_D S_0} \left( \frac{v}{v_s} \right)^2$$

from equations (5) and (7)

$$x_1 = \frac{(1-\eta)^2 \left(\frac{t}{t_0}\right)^6 + 2\eta(1-\eta) \left(\frac{t}{t_0}\right)^3 + \eta^2}{\left[1 + \frac{1}{M} \left[ \frac{(1-\eta)^2}{7} \left(\frac{t}{t_0}\right)^7 + \frac{\eta(1-\eta)}{2} \left(\frac{t}{t_0}\right)^4 + \eta^2 \frac{t}{t_0} \right] \right]^2} \quad (8)$$

III. Maximum Shock Force and Time of Occurrence During the Unfolding Phase

The time of occurrence of the maximum instantaneous shock factor,  $x_1$ , is difficult to determine for the general case. However, for  $\eta = 0$ , the maximum shock factor and time of occurrence are readily calculated. For  $\eta = 0$

$$x_1 = \frac{\left(\frac{t}{t_0}\right)^6}{\left[1 + \frac{1}{7M} \left(\frac{t}{t_0}\right)^7\right]^2}$$

Setting the derivative of  $x_1$  with respect to time equal to zero and solving for  $t/t_0$  at  $x_1$  max

$$\left(\frac{t}{t_0}\right) @ x_1 \text{ max} = \left(\frac{21M}{4}\right)^{\frac{1}{7}} \quad (9)$$

and the maximum shock factor is

$$x_1 \text{ max} = \frac{16}{49} \left(\frac{21M}{4}\right)^{\frac{6}{7}} \quad (10)$$

Equations (9) and (10) are valid for values of  $M \leq \frac{4}{21}$  (0.19), since for larger values of  $M$ , the maximum shock force occurs in the elastic phase of inflation.

Figures 9 and 10 illustrate the velocity and force profiles generated from equations (7) and (8) for initial projected area ratios of  $\eta = 0$ , and 0.2 with various mass ratios.

IV. Methods for Calculation of the Reference Time,  $t_0$

The ratio concept is an ideal method to analyze the effects of the various parameters on the velocity and force profiles of the opening parachutes; however, a means of calculating  $t_0$  is required before specific values can be computed. Methods for computing the varying mass flow into the inflating canopy mouth, the varying mass flow out through the varying inflated canopy surface area, and the volume of air,  $V_0$ , which must be collected during the inflation process are required.

Figure 11 represents a solid cloth-type parachute canopy at some instant during inflation. At any given instant, the parachute drag area is proportional to the maximum inflated diameter. Also, the maximum diameter in conjunction with the suspension lines determines the inflow mouth area (A-A) and the pressurized canopy area (B-B-B). This observation provided the basis for the following assumptions. The actual canopy shape is of minor importance.

a. The ratio of the instantaneous mouth inlet area to the steady-state mouth area is in the same ratio as the instantaneous drag area.

$$\frac{A_M}{A_{M0}} = \frac{C_D S}{C_D S_0}$$

b. The ratio of the instantaneous pressurized cloth surface area to the canopy surface area is in the same ratio as the instantaneous drag area.

$$\frac{S}{S_0} = \frac{C_D S}{C_D S_0}$$

c. Since the suspension lines in the unpressurized area of the canopy are straight, a pressure differential has not developed, and, therefore, the net airflow in this zone is zero.

Based on the foregoing assumptions, the mass flow equation can be written

$$dm = m \text{ inflow} - m \text{ outflow}$$

$$\rho \frac{dV}{dt} = \rho V A_M - \rho A_G P$$

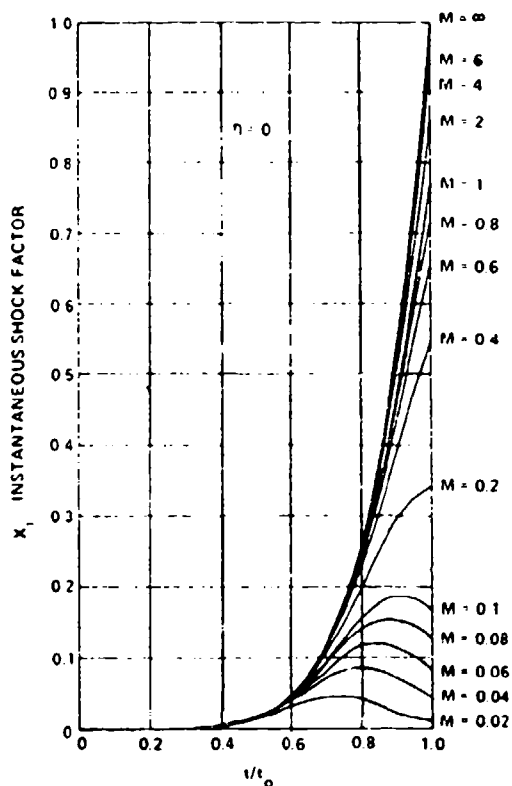
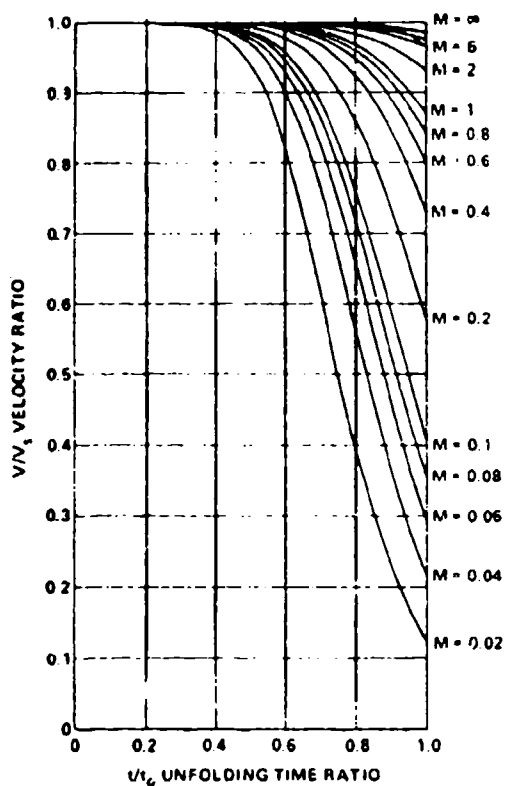


FIG. 9 EFFECT OF INITIAL AREA AND MASS RATIO ON THE SHOCK FACTOR AND VELOCITY RATIO DURING THE UNFOLDING PHASE FOR  $\eta = 0$ .

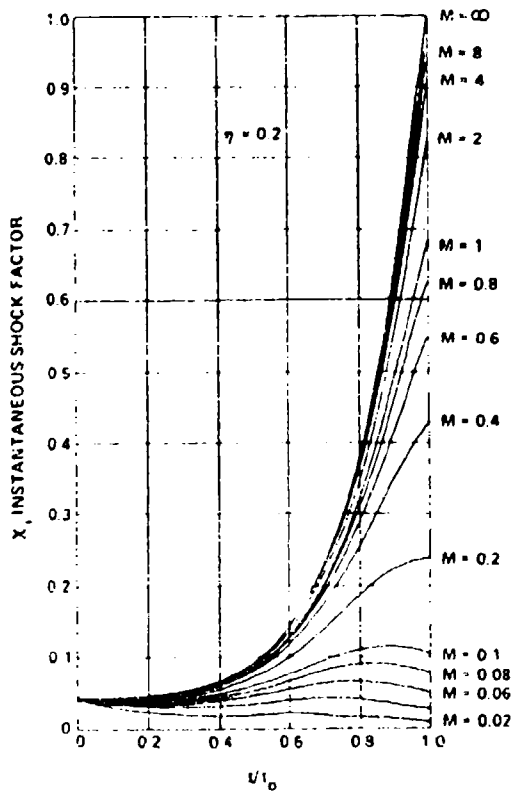
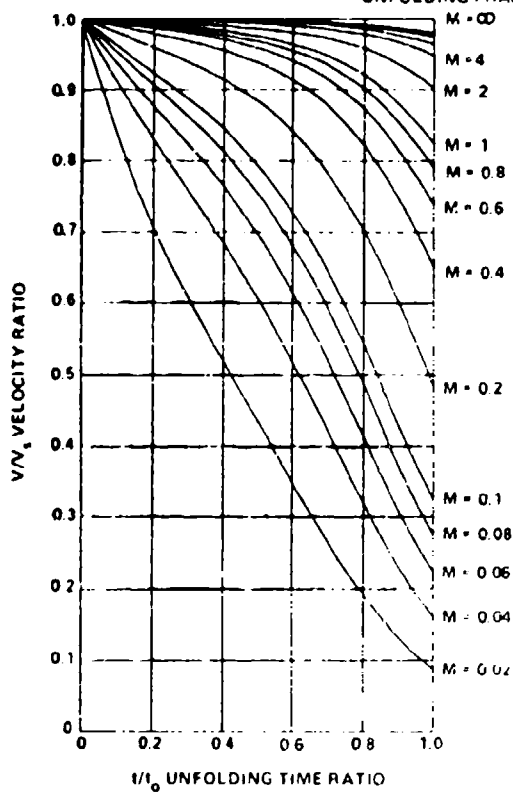


FIG. 10 EFFECT OF INITIAL AREA AND MASS RATIO ON THE SHOCK FACTOR AND VELOCITY RATIO DURING THE UNFOLDING PHASE FOR  $\eta = 0.2$ .

$$\rho \frac{dV}{dt} = \rho V A_{10} \frac{C_D S}{C_D S_0} - \rho A_{S0} \frac{C_B S}{C_D S_0} P \quad (11)$$

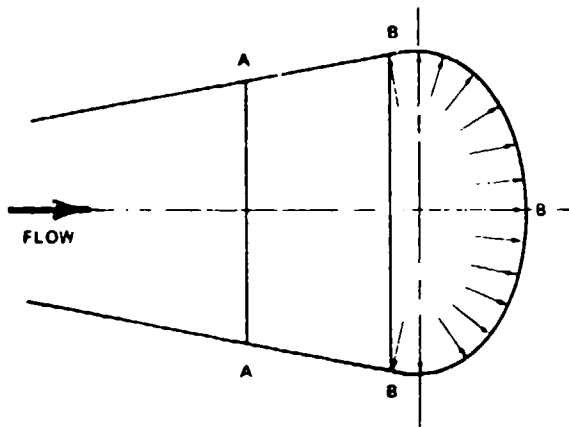


FIG. 11 PARTIALLY INFLATED PARACHUTE CANOPY

From equation (3)

$$\frac{C_D S}{C_D S_0} = \left(\frac{t}{t_0}\right)^6 ; \text{ for } n = 0$$

From equation (7)

$$V = \frac{V_B}{1 + \frac{1}{7M} \left(\frac{t}{t_0}\right)^7} ; n = 0$$

From equation (26)

$$P = k \left(\frac{C_B S}{C_D S_0}\right)^n \quad (12)$$

$$-A_{S0} k \left(\frac{C_B S}{C_D S_0}\right)^n \int_0^{t_0} \left(\frac{t}{t_0}\right)^6 \left[ \frac{V_S}{1 + \frac{1}{7M} \left(\frac{t}{t_0}\right)^7} \right]^{2n} dt \quad (12)$$

Integrating:

$$\underline{V}_0 = A_{M0} V_S t_0 M \ln \left[ 1 + \frac{1}{7M} \right]$$

$$-A_{S0} k \left(\frac{C_B S}{C_D S_0}\right)^n \int_0^{t_0} \left(\frac{t}{t_0}\right)^6 \left[ \frac{V_S}{1 + \frac{1}{7M} \left(\frac{t}{t_0}\right)^7} \right]^{2n} dt \quad (13)$$

Measured values of n indicate a data range from 0.574 through 0.771. A convenient solution to the reference time equation evolves when n is assigned a value of 1/2. Integrating equation (13) and using

$$V_S t_0 M = \frac{2W}{\rho C_D S_0}$$

$$\text{LET } K_1 = \frac{\rho V_S^2}{2W} \left[ \frac{C_D S_0}{A_{M0} - A_{S0} k \left(\frac{C_B S}{C_D S_0}\right)^{1/2}} \right]$$

$$t_0 = \frac{14W}{\rho V_S C_D S_0} \left[ e^{K_1} - 1 \right] \quad (14)$$

Equation (14) expresses the unfolding reference time,  $t_0$ , in terms of mass, altitude, snatch velocity, airflow characteristics of the cloth, and the steady-state parachute geometry. Note that the term  $\rho V_S^2 / W$  is the ratio of the included air mass to the mass of the retarded hardware. Multiplying both sides of equation (14) by  $V_S$  demonstrates that

$$V_S t_0 = \text{a constant which is a function of altitude}$$

Figures 12 and 13 indicate the parachute unfolding time and unfolding distance for values of  $n = 1/2$  and  $n = 0.63246$ . Note the variation and convergence with rising altitude. The opening shock force is strongly influenced by the inflation time. Because of this, the

$$\int_0^{\underline{V}_0} dV = A_{M0} V_S \int_0^{t_0} \frac{\left(\frac{t}{t_0}\right)^6}{1 + \frac{1}{7M} \left(\frac{t}{t_0}\right)^7} dt$$

value of  $t_0$  calculated by using a realistic value of  $n$  should be used in the lower atmosphere.

As an example of this method of opening-shock analysis, let us examine the effect of altitude on the opening-shock force of a T-10-type parachute retarding a 200-pound weight from a snatch velocity of  $V_s = 400$  feet per second at sea level. Conditions of constant velocity and constant dynamic pressure are investigated. The results are presented in Figure 14. At low altitudes, the opening-shock force is less than the steady-state drag force; however, as altitude rises, the opening shock eventually exceeds the steady-state drag force at some altitude. This trend is in agreement with field test observations.

V. Correction of  $t_0$  for Initial Area Effects

The unfolding reference time,  $t_0$ , calculated by the previous methods assumes that the parachute inflates from zero drag area. In reality, a parachute has a drag

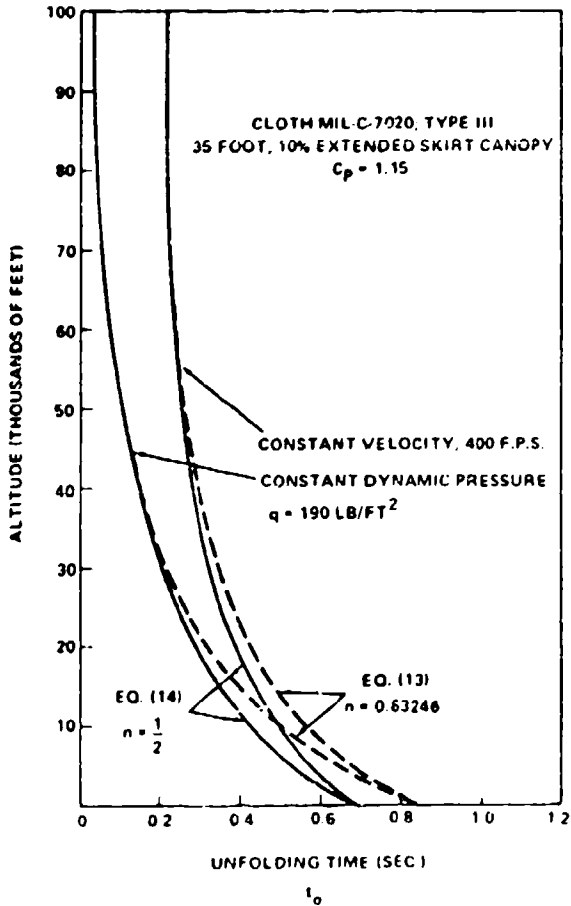


FIG. 12 EFFECT OF ALTITUDE ON THE UNFOLDING TIME " $t_0$ " AT CONSTANT VELOCITY AND CONSTANT DYNAMIC PRESSURE FOR  $n = 1/2$  AND  $n = 0.63296$

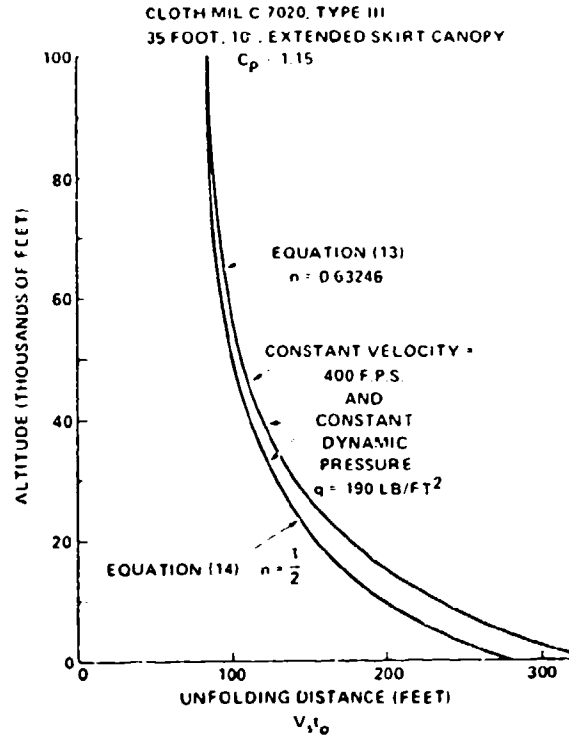


FIG. 13 EFFECT OF ALTITUDE ON THE UNFOLDING DISTANCE AT CONSTANT VELOCITY AND CONSTANT DYNAMIC PRESSURE FOR  $n = 1/2$  AND  $n = 0.63246$ .

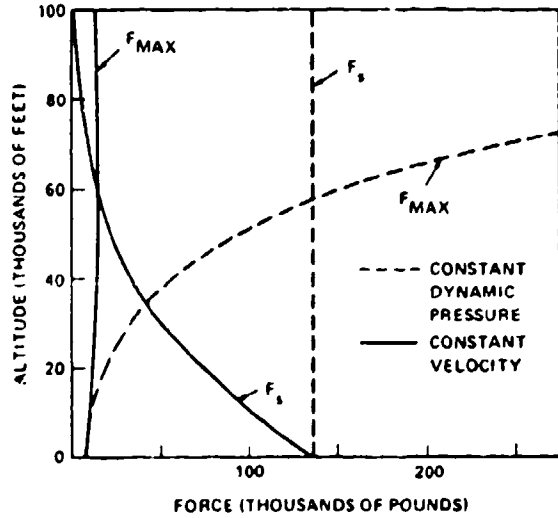


FIG. 14 VARIATION OF STEADY STATE DRAG,  $F_s$ , AND MAXIMUM OPENING SHOCK WITH ALTITUDE FOR CONSTANT VELOCITY AND CONSTANT DYNAMIC PRESSURE

area at the beginning of inflation. Once  $t_0$  has been calculated, a correction can be applied, based upon what is known about the initial conditions.

Case A - When the initial projected area is known

$$\frac{a_i}{a_c} = \left(\frac{t_i}{t_c}\right)^3$$

$$t_i = \left(\frac{a_i}{a_c}\right)^{1/3} t_{o\text{calculated}}$$

$$t_{o\text{corrected}} = \left[1 - \left(\frac{a_i}{a_c}\right)^{1/3}\right] t_{o\text{calculated}} \quad (15)$$

Case B - When the initial drag area is known

$$\frac{C_D S_i}{C_D S_o} = \left(\frac{t_i}{t_o}\right)^6$$

$$t_i = \left(\frac{C_D S_i}{C_D S_o}\right)^{1/6} t_{o\text{calculated}}$$

$$t_{o\text{corrected}} = \left[1 - \left(\frac{C_D S_i}{C_D S_o}\right)^{1/6}\right] t_{o\text{calculated}} \quad (16)$$

The mass ratio should now be adjusted for the corrected  $t_o$  before velocity and force profiles are determined.

#### VI. Opening-Shock Force, Velocity Ratio, and Inflation Time During the Elastic Phase of Parachute Inflation

The mass ratio,  $M$ , is an important parameter in parachute analysis. For values of  $M \ll 4/21$ , the maximum opening-shock force occurs early in the inflation process, and the elastic properties of the canopy are not significant. As the mass ratio approaches  $M = 4/21$ , the magnitude of the opening-shock force increases, and the time of occurrence happens later in the deployment sequence. For mass ratios  $M > 4/21$ , the maximum shock force will occur after the reference time,  $t_o$ . Parachutes designed for high mass ratio operation must provide a structure of sufficient constructed strength,  $F_c$ , so that the actual elongation of the canopy under load is less

than the maximum extensibility,  $e_{\text{max}}$ , of the materials.

Development of the analysis in the elastic phase of inflation is similar to the technique used in the unfolding phase. Newton's second law of motion is used, together with the drag area ratio signature and mass ratio

$$\frac{C_D S}{C_D S_o} = \left(\frac{t}{t_o}\right)^6$$

which is still valid, as shown in Figure 7

$$\frac{1}{M t_o} \int_{t_o}^t \left(\frac{t}{t_o}\right)^6 dt = v_s \int_{v_o}^v \frac{-dv}{v^2}$$

Integrating and solving for  $\frac{v}{v_s}$

$$\frac{v}{v_s} = \frac{1}{\frac{v_s}{v_o} + \frac{1}{7M} \left[ \left(\frac{t}{t_o}\right)^7 - 1 \right]} \quad (17)$$

where  $\frac{v_o}{v_s}$  is the velocity ratio of the unfolding process at time  $t = t_o$ .

$$\frac{v_o}{v_s} = \frac{1}{1 + \frac{1}{M} \left[ \frac{(1-\eta)^2}{7} + \frac{\eta(1-\eta)}{2} + \eta^2 \right]} \quad (18)$$

The instantaneous shock factor in the elastic phase becomes

$$x_1 = \frac{C_D S}{C_D S_o} \left(\frac{v}{v_s}\right)^2$$

$$x_1 = \frac{\left(\frac{t}{t_o}\right)^6}{\left[ \frac{v_o}{v_s} + \frac{1}{7M} \left[ \left(\frac{t}{t_o}\right)^7 - 1 \right] \right]^2} \quad (19)$$

The end point of the inflation process depends upon the applied loads, elasticity of the canopy, and the constructed strength of the parachute. A linear load elongation

relationship is utilized to determine the maximum drag area.

$$\frac{c}{F} = \frac{\epsilon_{max}}{F_c}$$

$$c = \frac{F \epsilon_{max}}{F_c} \quad (20)$$

The force, F, is initially the instantaneous force at the end of the unfolding process

$$F = X_0 F_s \quad (21)$$

where  $X_0$  is the shock factor of the unfolding phase at  $t = t_0$

$$X_0 = \left[ \frac{1}{1 + \frac{1}{M} \left[ \frac{(1-\eta)^2}{7} + \frac{\eta(1-\eta)}{2} + \eta^2 \right]} \right]^2 \quad (22)$$

Since the inflated shape is defined, the drag coefficient is considered to be constant, and the instantaneous force is proportional to the dynamic pressure and projected area. The maximum projected area would be developed if the dynamic pressure remained constant during the elastic phase. Under very high mass ratios, this is nearly the case over this very brief time period; but as the mass ratio decreases, the velocity decay has a more significant effect. The simplest approach for all mass ratios is to determine the maximum drag area of the canopy as if elastic inflation had occurred at constant dynamic pressure. Then utilizing the time ratio determined as an end point, intermediate shock factors can be calculated from equation (19) and maximum force assessed.

The initial force,  $X_0 F_s$ , causes the canopy to increase in projected area. The new projected area in turn increases the total force on the canopy which produces a secondary projected area increase. The resulting series of events are resisted by the parachute materials. The parachute must, therefore, be constructed of sufficient strength to prevent the elongation of the materials from exceeding the maximum elongation.

$$\epsilon_0 = \frac{X_0 F_s}{F_c} \epsilon_{max} \quad (23)$$

The next force in the series at constant q

$$F_1 = X_0 F_s \frac{A_1}{A_c}$$

where

$$\frac{A_1}{A_c} = (1 + \epsilon_0)^2$$

Subsequent elongations in the system can be shown to be

$$\epsilon_1 = \epsilon_0 (1 + \epsilon_0)^2$$

$$\epsilon_2 = \epsilon_0 (1 + \epsilon_0 (1 + \epsilon_0)^2)^2$$

The required canopy constructed strength can be determined for a given set of deployment conditions. The limiting value of the series ( $\epsilon_l$ ) determines the end point time ratio.

$$\left( \frac{t_f}{t_0} \right)^6 = \frac{C_{D S_{max}}}{C_{D S_0}} = (1 + \epsilon_l)^2$$

$$\left( \frac{t_f}{t_0} \right) = \left( \frac{C_{D S_{max}}}{C_{D S_0}} \right)^{1/6} = (1 + \epsilon_l)^{1/3} \quad (24)$$

Figure 15 illustrates the maximum drag area ratio as a function of  $\epsilon_0$ .

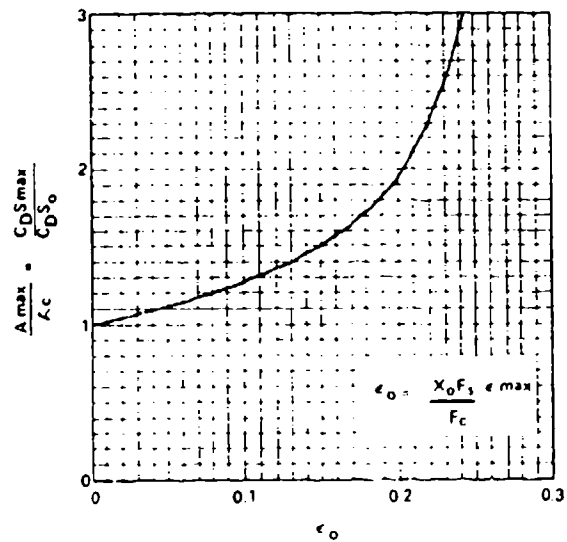


FIG. 15 MAXIMUM DRAG AREA RATIO VS. INITIAL ELONGATION

VII. Application of Cloth Permeability to the Calculation of the Inflation Time of Solid Cloth Parachutes

The mass outflow through the pressurized region of an inflating solid cloth parachute at any instant is dependent upon the canopy area which is subjected to airflow and the rate of airflow through that area. The variation of pressurized area as a function of reference time,  $t_0$ , was earlier assumed to be proportional to the instantaneous drag area ratio, leaving the rate-of-airflow problem to solve. The permeability parameter of cloth was a natural choice for determining the rate of airflow through the cloth as a function of pressure differential across the cloth. Heretofore, these data have been more of a qualitative, rather than quantitative, value. A new method of analysis was developed wherein a generalized curve of the form  $P = k(\Delta P)^n$  was fitted to cloth permeability data for a number of different cloths and gives surprisingly good agreement over the pressure differential range of available data. The pressure differential was then related to the trajectory conditions to give a generalized expression which can be used in the finite mass ratio range, as well as the infinite mass case. The permeability properties were transformed into a mass flow ratio,  $M'$ , which shows agreement with the effective porosity concept.

Measured and calculated permeability pressure data for several standard cloths are illustrated in Figure 16. This method has been applied to various types of cloth between the extremes of a highly permeable 3-momme silk to a relatively impervious parachute pack container cloth with reasonably good results, see Figure 17.

The canopy pressure coefficient,  $C_p$ , is defined as the ratio of the pressure differential across the cloth to the dynamic pressure of the free stream.

$$C_p = \frac{\Delta P}{q} = \frac{P(\text{internal}) - P(\text{external})}{1/2 \rho V^2} \quad (25)$$

where  $V$  is based on equation (7).

The permeability expression,  $P = k(\Delta P)^n$  becomes

$$P = k(C_p \frac{\rho V^2}{2})^n \quad (26)$$

Although some progress has been made by Melzig and others on the measurement of the variation of the pressure coefficient on an actual inflating canopy, this dimension and its variation with time are still dark areas at the time of this writing. At the present time, a constant average value of pressure coefficient is

used in these calculations. Figure 18 presents the effect of pressure coefficient and altitude on the unfolding time for constant deployment conditions.

It is well known that the inflation time of solid cloth parachutes decreases as the operational altitude increases. This effect can be explained by considering the ratio of the mass outflow through a unit cloth area to the mass inflow through a unit mouth area.

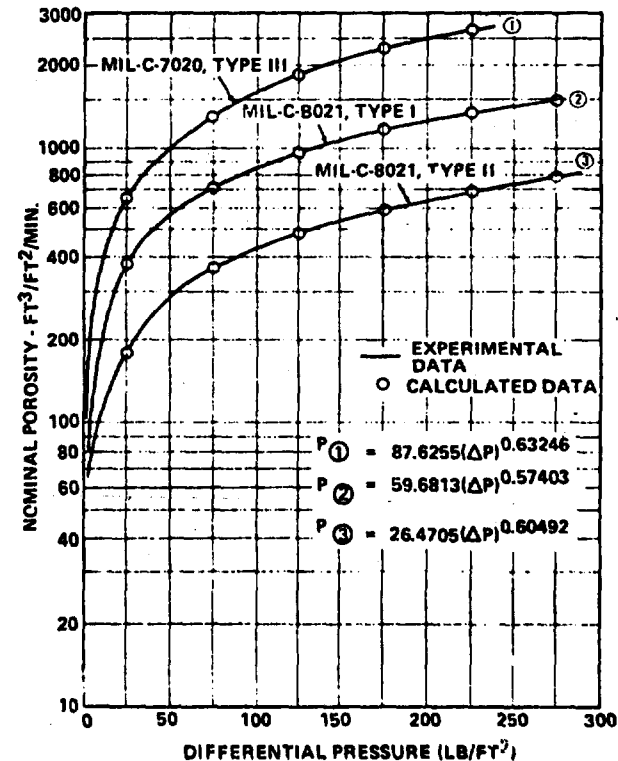
$$M' = \text{mass flow ratio} = \frac{\text{mass outflow}}{\text{mass inflow}}$$

where

$$\text{mass outflow} = P \frac{\text{slugs}}{\text{ft}^2\text{-sec}} \text{ (per ft}^2 \text{ cloth area)}$$

and

$$\text{mass inflow} = V \frac{\text{slugs}}{\text{ft}^2\text{-sec}} \text{ (per ft}^2 \text{ inflow area)}$$



REPRODUCED FROM REFERENCE (4)

FIG. 16 NOMINAL POROSITY OF PARACHUTE MATERIAL VS DIFFERENTIAL PRESSURE.

Therefore, the mass flow ratio becomes

$$M' = \frac{P \rho}{V \rho} = \frac{P}{V}$$

$$M' = k \left( \frac{C_p \rho}{2} \right)^n v^{(2n-1)} \quad (27)$$

Effective porosity,  $C$ , is defined as the ratio of the velocity through the cloth,  $u$ , to a fictitious theoretical velocity,  $v$ , which will produce the particular  $\Delta P = 1/\rho v^2$ .

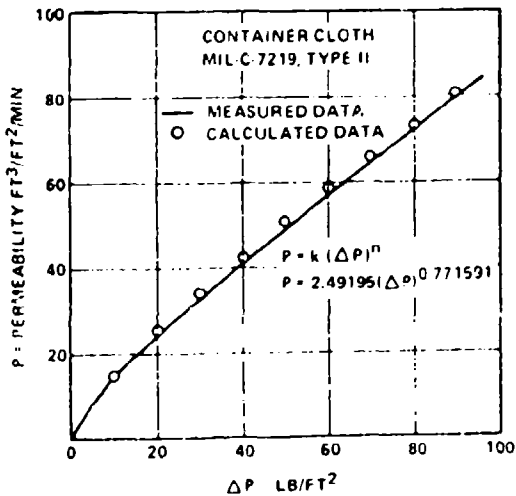
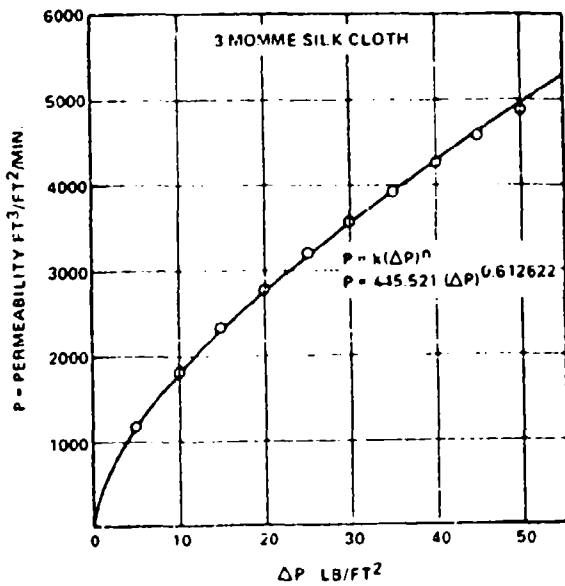


FIG. 17 COMPARISON OF MEASURED AND CALCULATED PERMEABILITY FOR RELATIVELY PERMEABLE AND IMPERMEABLE CLOTHS

AVERAGE CANOPY PRESSURE COEFFICIENT DURING INFLATION INCLUDING THE VENT

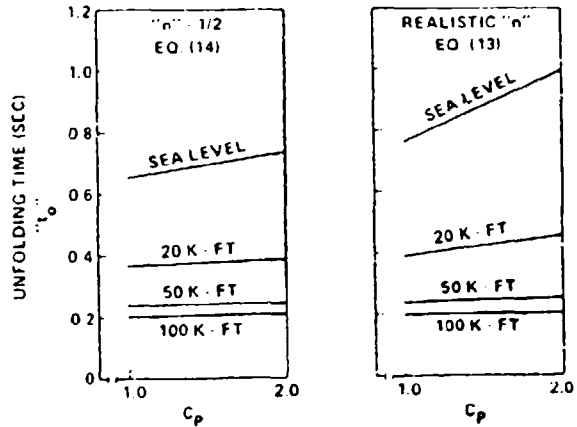
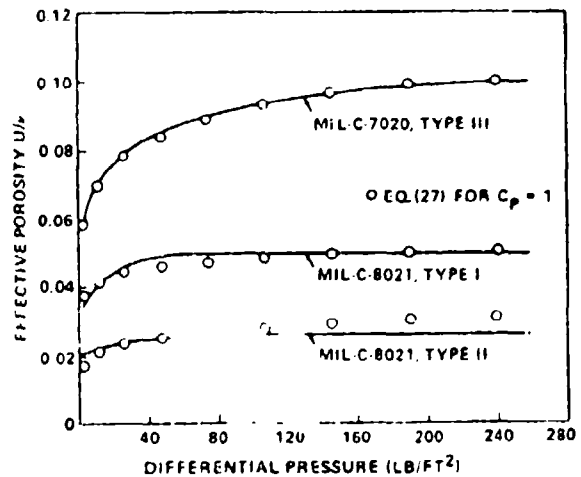


FIG. 18 EFFECT OF PRESSURE COEFFICIENT AND ALTITUDE ON THE UNFOLDING TIME.

$$\text{effective porosity, } C = \frac{u}{v} \quad (28)$$

Comparison of the mass flow ratio and previously published effective porosity data is shown in Figure 19. The effects of altitude and velocity on the mass flow ratio are presented in Figures 20, and 21 for constant velocity and constant altitude. The decrease of cloth permeability with altitude is evident.

The permeability constants "k" and "n" can be determined from the permeability pressure differential data as obtained from an instrument such as a Frazier Permeometer. Two data points, "A" and



REPRODUCED FROM REFERENCE (4)

FIG. 19 THE EFFECTIVE POROSITY OF PARACHUTE MATERIALS VS. DIFFERENTIAL PRESSURE

"B," are selected in such a manner that point "A" is in a low-pressure zone below the knee of the curve, and point "B" is located in the upper end of the high-pressure zone, as shown in Figure 22.

The two standard measurements of 1/2 inch of water and 20 inches of water appear to be good data points if both are

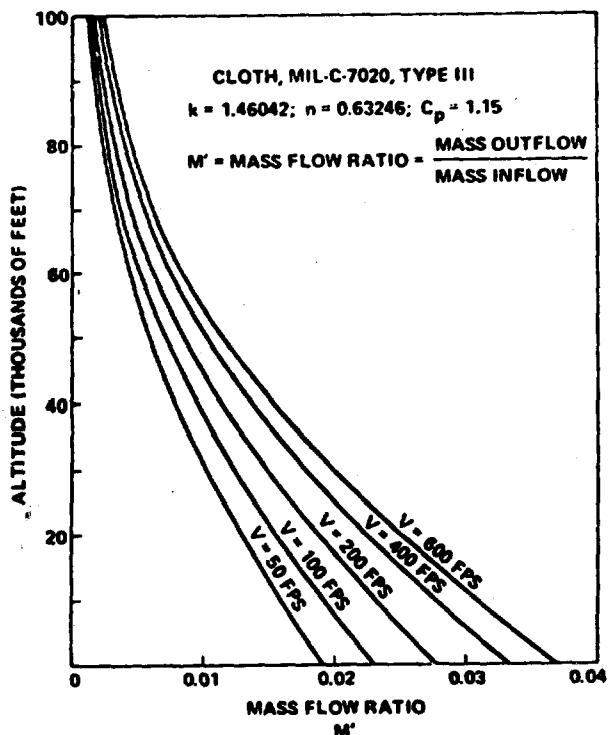


FIG. 20 EFFECT OF ALTITUDE ON MASS FLOW RATIO AT CONSTANT VELOCITY

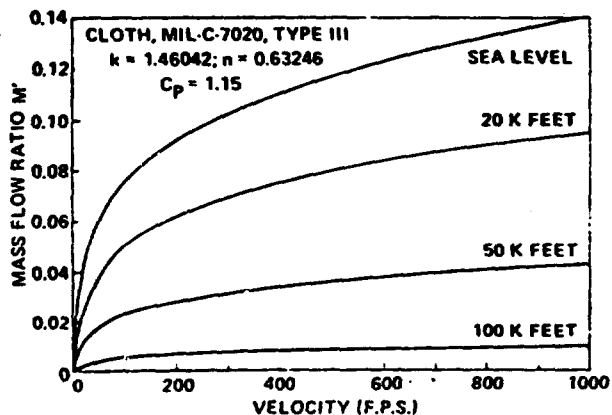


FIG. 21 EFFECT OF VELOCITY ON MASS FLOW RATIO AT CONSTANT DENSITY

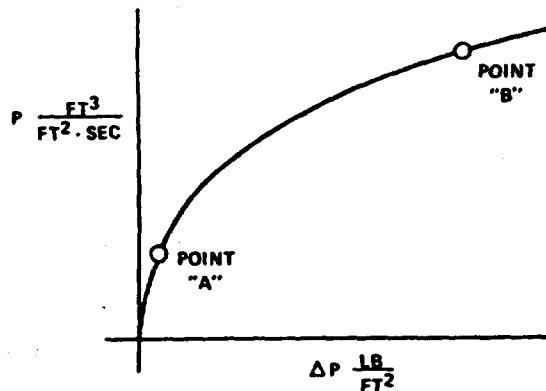


FIG. 22 LOCATION OF DATA POINTS FOR DETERMINATION OF "k" AND "n"

available on the same sample. Substituting the data from points "A" and "B" into  $P = k(\Delta P)^n$ :

$$n = \frac{\ln\left(\frac{P_B}{P_A}\right)}{\ln\left(\frac{\Delta P_B}{\Delta P_A}\right)} \quad (29)$$

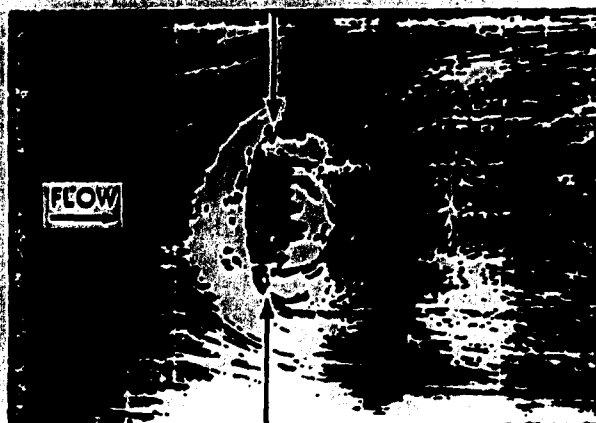
$$k = \frac{P_A}{(\Delta P_A)^n} = \frac{P_B}{(\Delta P_B)^n} \quad (30)$$

#### VIII. Determination of the Parachute Included Volume and Associated Air Mass

Before the reference time,  $t_0$ , and inflation time,  $t_f$ , can be calculated, the volume of atmosphere,  $V_0$ , which is to be collected during the inflation process must be accurately known. This requirement dictates that a realistic inflated canopy shape and associated volume of atmosphere be determined. Figure 23 was reproduced from reference (5). The technique of using lampblack coated plates to determine the airflow patterns around metal models of inflated canopy shapes was used by the investigator of reference (5) to study the stability characteristics of contemporary parachutes, i.e., 1943. A by-product of this study is that it is clearly shown that the volume of air within the canopy bulges out of the canopy mouth (indicated by arrows) and extends ahead of the canopy hem. This volume must be collected during the inflation process. Another neglected, but significant, source of canopy volume exists in the billowed portion of the gore panels.



HEMISPHERE



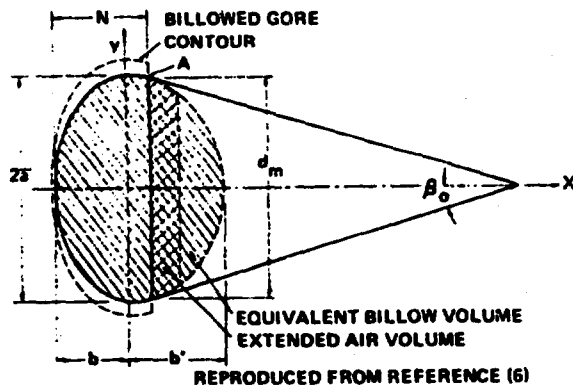
VENT PARACHUTE

REPRODUCED FROM REFERENCE (5)

FIG. 23 AIRFLOW PATTERNS SHOWING AIR VOLUME  
AHEAD OF CANOPY HEM

The steady-state canopy shape has been observed in wind-tunnel and field tests to be elliptical in profile. Studies of the inflated shape and included volume of several parachute types (flat circular, 10 percent extended skirt, elliptical, hemispherical, ring slot, ribbon, and cross) are documented in references (6) and (7). These studies demonstrated that the steady-state profile shape of inflated canopies of the various types can be approximated to be two ellipses of common major diameter,  $2\bar{a}$ , and dissimilar minor diameters,  $b$  and  $b'$ , as shown in Figure 24. It was also shown that the volume of the ellipsoid of revolution formed by revolving the profile shape about the canopy axis was a good approximation of the volume of atmosphere to be collected during canopy inflation and included the air volume extended ahead of the parachute skirt hem together with the billowed gore volume.

$$\underline{V}_o = \frac{2}{3} \pi \bar{a}^3 \left[ \frac{b}{\bar{a}} + \frac{b'}{\bar{a}} \right] \quad (31)$$



REPRODUCED FROM REFERENCE (6)

FIG. 24 PARACHUTE CROSS SECTION NOMENCLATURE

Tables I and II are summaries of test results reproduced from references (6) and (7), respectively, for the convenience of the reader.

#### IX. References

1. "A Method to Reduce Parachute Inflation Time with a Minor Increase in Opening Force," WADD Report TR 60-761
2. Berndt, R. J., and DeWesse, J. H., "Filling Time Prediction Approach for Solid Cloth Type Parachute Canopies," AIAA Aerodynamic Deceleration Systems Conference, Houston, Texas, 7-9 Sep 1966
3. "Theoretical Parachute Investigations," Progress Report No. 4, Project No. 5, WADC Contract AF33 (616)-3955, University of Minnesota
4. "Performance of and Design Criteria for Deployable Aerodynamic Decelerators," TR ASK-TR-61-579, AFFDL, AIRFORCESYSCOM, Dec 1963
5. "Investigation of Stability of Parachutes and Development of Stable Parachutes from Fabric of Normal Porosity," Count Zeppelin Research Institute Report No. 300, 23 Mar 1943
6. Ludtke, W. P., "A New Approach to the Determination of the Steady-State Inflated Shape and Included Volume of Several Parachute Types," NOLTR 69-159, 11 Sep 1969
7. Ludtke, W. P., "A New Approach to the Determination of the Steady-State Inflated Shape and Included Volume of Several Parachute Types in 24-Gore and 30-Gore Configurations," NOLTR 70-178, 3 Sep 1970

**TABLE I SUMMARY OF PARACHUTE SHAPE TEST RESULTS  
FOR 12-GORE AMD 16-GORE CONFIGURATIONS**

Parachute Type	No of Gores	Suspension Line Length inches	Velocity		Scale Factor K				$\frac{N}{S}$	Axes Ratio				Volume in <sup>3</sup>			$\frac{V_o}{V_H}$
			mph	fps	$\frac{2z}{D_o}$	$\frac{2z}{D_f}$	$\frac{2z}{D_R}$	$\frac{2z}{L}$		$\frac{b}{a}$	$\frac{b}{s}$	$\frac{b}{a} \cdot \frac{b}{s}$	$V_H$	$V_C$	$V_o$		
Flat Circular	12	34	50	73	645	650			856	6115	8817	1 4932	4476	4481	6980	1.56	
	16	34	50	73	663	669			820	5558	9039	1 4597	4450	4100	7325	1.65	
10% Extended Skirt	12	34	100	147	663	652			881	6424	8860	1 5284	3928	4400	6783	1.73	
	16	34	17	25	654	640			785	5580	8502	1 4082	4051	3985	6197	1.53	
Elliptical	12	34	75	110			916		812	5626	9657	1 5283		3322	5405		
	16	34	17	25			875		800	6169	8163	1 4332		2726	4405		
Hemispherical	12	34	125	183			996		1 254	1 0005	9080	1 9085		6224	8666		
	16	34	75	110			994		1 185	9129	9380	1 8509		5921	8370		
Ring Slot 16% Geometric Porosity	12	34	25	37	607	654			853	6566	8735	1 530	3800	3650	5903	1.55	
	12	34	100	147	616	663			922	6566	8735	1 530	3800	4198	6166	1.62	
	12	34	200	293	637	686			918	6566	8735	1 530	3800	4624	6826	1.90	
	16	34	25	37	611	658			827	6004	8890	1 4894	3800	3763	5685	1.50	
	16	34	100	147	617	664			864	6004	8890	1 4894	3800	3985	6030	1.59	
	16	34	200	293	645	695			844	6004	8890	1 4894	3800	4430	6897	1.82	
Ribbon 24% Geometric Porosity	12	34	25	37	586	632			859	6558	8768	1 5326	3800	3323	5335	1.40	
	12	34	100	147	615	663			837	6558	8768	1 5326	3800	3714	6163	1.62	
	12	34	200	293	632	681			877	6558	8768	1 5326	3800	4280	6683	1.76	
	16	34	25	37	603	650			797	5570	8578	1 4148	3800	3438	5358	1.41	
	16	34	100	147	626	674			791	5570	8578	1 4148	3800	3804	5983	1.57	
	16	34	200	293	648	698			781	5570	8578	1 4148	3800	4164	6656	1.75	
Cross Chute W/L = 264		34	25	37	710		543	1 242		8867	1 2776	2 1643	1928	3768	5798	3.01	
		34	100	147	707		540	1 270		8867	1 2776	2 1643	1928	3810	5712	2.96	
		34	200	293	716		547	1 285		8867	1 2776	2 1643	1928	4212	5925	3.07	
		47	25	37	759		580	1 113		8494	1 2512	2 1006	1928	4052	6868	3.56	
		47	100	147	729		557	1 205		8494	1 2512	2 1006	1928	3973	5958	3.09	
		47	200	293	775		592	1 110		8494	1 2512	2 1006	1928	4292	7303	3.79	

REPRODUCED FROM REFERENCE (6)

**TABLE II SUMMARY OF PARACHUTE SHAPE TEST RESULTS  
FOR 24-GORE AND 30-GORE CONFIGURATIONS**

Parachute Type	No of Gores	Suspension Line Length inches	Velocity		Scale Factor K				$\frac{N}{S}$	Axes Ratio				Volume in <sup>3</sup>			$\frac{V_o}{V_H}$
			mph	fps	$\frac{2z}{D_o}$	$\frac{2z}{D_f}$	$\frac{2z}{D_R}$	$\frac{2z}{L}$		$\frac{b}{a}$	$\frac{b}{s}$	$\frac{b}{a} \cdot \frac{b}{s}$	$V_H$	$V_C$	$V_o$		
Flat Circulars	24	34	50	73	677	679			795	5758	8126	1 3884	4362	4695	7277	1.67	
	30	34	17	25	668	669			827	6214	7806	1 4020	4342	4626	7027	1.62	
10% Extended Skirt	24	34	100	147	665	648			834	5949	8771	1 4720	4138	4446	6930	1.67	
	30	34	17	25	650	633			825	6255	7962	1 4127	4172	4076	6265	1.50	
Ring Slot 16% Geometrically Porous	24	34	25	37	663	665			824	5800	9053	1 4853	3591	3878	6031	1.68	
	24	34	100	147	680	682			819	5800	9053	1 4853	3591	4079	6510	1.81	
	24	34	200	293	694	696			809	5800	9053	1 4853	3591	4270	6924	1.93	
	30	34	25	37	677	678			788	5800	9053	1 4853	3582	3826	6404	1.79	
	30	34	100	147	684	685			807	5800	9053	1 4853	3582	4023	6588	1.84	
	30	34	200	293	698	699			800	5800	9053	1 4853	3582	4260	7012	1.96	
Ribbon 24% Geometrically Porous	24	34	25	37	671	673			770	5980	8187	1 4167	3591	3591	5968	1.66	
	24	34	100	147	676	678			813	5980	8187	1 4167	3591	3927	6097	1.70	
	24	34	200	293	687	689			804	5980	8187	1 4167	3591	4061	6389	1.79	
	30	34	25	37	655	657			782	6021	8463	1 4484	3582	3396	5666	1.58	
	30	34	100	147	669	670			784	6021	8463	1 4484	3582	3622	6022	1.68	
	30	34	200	293	677	679			823	6021	8463	1 4484	3582	4002	6256	1.75	

\*Since this parachute was breathing during the test, several photographs were taken at each speed. The data were reduced from the photograph which most reasonably appeared to represent the equilibrium state.

REPRODUCED FROM REFERENCE (7)

## X. List of Symbols

$A_c$	- Steady-state projected area of the inflated parachute, $ft^2$	$P$	- Cloth permeability - rate of air-flow through a cloth at an arbitrary differential pressure, $ft^3/ft^2/sec$
$A_{t1}$	- Instantaneous canopy mouth area, $ft^2$	$q$	- Dynamic pressure, $lb/ft^2$
$A_{No}$	- Steady-state inflated mouth area, $ft^2$	$S$	- Instantaneous inflated canopy surface area, $ft^2$
$a$	- Acceleration, $ft/sec^2$	$S_o = A_{so}$	- Canopy surface area, $ft^2$
$2\bar{a}$	- Maximum inflated parachute diameter of gore mainseam, $ft$	$t$	- Instantaneous time, $sec$
$b$	- Minor axis of the ellipse bounded by the major axis ( $2\bar{a}$ ) and the vent of the canopy, $ft$	$t_o$	- Reference time when the parachute has reached the design drag area for the first time, $sec$
$b'$	- Minor axis of the ellipse which includes the skirt hem of the canopy, $ft$	$t_f$	- Canopy inflation time when the inflated canopy has reached its maximum physical size, $sec$
$C$	- Effective porosity	$u$	- Air velocity through cloth in effective porosity, $ft/sec$
$C_D$	- Parachute coefficient of drag	$v$	- Fictitious theoretical velocity used in effective porosity, $ft/sec$
$C_P$	- Parachute pressure coefficient, relates internal and external pressure ( $\Delta P$ ) on canopy surface to the dynamic pressure of the free stream	$V$	- Instantaneous system velocity, $ft/sec$
$D_o$	- Nominal diameter of the aerodynamic decelerator = $\sqrt{4S_o/\pi}$ , $ft$	$V_o$	- System velocity at the time $t = t_o$ , $ft/sec$
$F$	- Instantaneous force, $lbs$	$V_s$	- System velocity at the end of suspension line stretch, $ft/sec$
$F_s$	- Steady-state drag force that would be produced by a fully open parachute at velocity $V_s$ , $lbs$	$\underline{V}_o$	- Volume of air which must be collected during the inflation process, $ft^3$
$F_c$	- Constructed strength of the parachute, $lbs$	$W$	- Hardware weight, $lb$
$F_{max}$	- Maximum opening-shock force, $lbs$	$x_t$	- Instantaneous shock factor
$g$	- Gravitational acceleration, $ft/sec^2$	$X_o$	- Shock factor at the time $t = t_o$
$k$	- Permeability constant of canopy cloth	$\rho$	- Air density, $slugs/ft^3$
$m$	- Mass, $slugs$	$\eta$	- Ratio of parachute projected mouth area at line stretch to the steady-state projected area
$M$	- Mass ratio - ratio of the mass of the retarded hardware (including parachute) to a mass of atmosphere contained in a right circular cylinder of length ( $V_s t_o$ ), face area ( $C_D S_o$ ), and density ( $\rho$ )	$\epsilon$	- Instantaneous elongation
$M'$	- Mass flow ratio - ratio of atmosphere flowing through a unit cloth area to the atmosphere flowing through a unit inlet area at arbitrary pressure	$\epsilon_{max}$	- Maximum elongation
$n$	- Permeability constant of canopy cloth	$\epsilon_o$	- Initial elongation at the beginning of the elastic phase of inflation
		S.F.	- Parachute safety factor = $F_c/F_{max}$

## Appendix B

## A GUIDE FOR THE USE OF APPENDIX A

At first reading, Appendix A may appear to be a complicated system of analysis because of the many formulae presented. Actually, once understood, the technique is straightforward and uncomplicated. The author has attempted to simplify the algebra wherever possible. This appendix presents, in semi-outline form, a guide to the sequence of calculations because the analysis does require use of formulae from the text, not necessarily in the order in which they were presented. Also, the user can be referred to graphs of performance to illustrate effects.

In order to compute  $t_0$ , other parameters must be obtained from various sources.

## I. Determine System Parameters

1.  $C_D S_0$ , drag area,  $\text{ft}^2$  obtained from design requirement.
2.  $V_s$ , fps, velocity of system at suspension line stretch.
3.  $\rho$ , slugs/ $\text{ft}^3$ , air density at deployment altitude.
4.  $W$ , lb, system weight (including weight of the parachute) from design requirements.
5.  $V_0$ ,  $\text{ft}^3$ , this volume of air, which is to be collected during inflation, is calculated from the steady-state inflated shape geometry of the particular parachute type. The nomenclature is described in Figure 24, p. A-14. When  $D_0$  or  $D_p$  is known,  $\bar{a}$  can be calculated from data in Table I and Table II, p. A-15, for various parachute types and number of gores. Then the geometric volume  $V_0$  can be calculated by Equation (31), p. A-14, with appropriate values of  $b/\bar{a}$  and  $b'/\bar{a}$  from the tables.
6.  $A_{MO}$ ,  $\text{ft}^2$ , steady-state canopy mouth area

$$A_{MO} = \pi \bar{a}^2 \left[ 1 - \left( \frac{N/\bar{a} - b/\bar{a}}{b'/\bar{a}} \right)^2 \right] \quad (\text{B.1})$$

where  $N/\bar{a}$ ,  $b/\bar{a}$ , and  $b'/\bar{a}$  are available from Tables I and II for the particular type of parachute and number of gores.

$$7. A_{SO}, \text{ ft}^2, \text{ canopy surface area} = \frac{\pi}{4} D_0^2$$

8.  $C_p$ , pressure coefficient, see Figure 18, p. A-12. A constant  $C_p = 1.7$  for all altitudes seems to yield acceptable results.

9. Constants  $k$  and  $n$  are derived from measurements of the air flow through the cloth. Only  $k$  is needed for Equation (14), but  $n$  is also required for Equation (13). These parameters can be determined for any cloth using the technique described beginning on p. A-12. The two-point method is adequate if the  $\Delta P$  across the cloth is in the range of  $\Delta P$  for actual operation. Check-points of cloth permeability can be measured and compared to calculated values to verify agreement. If the data are to be extrapolated to operational  $\Delta P$ 's greater than measured, a better method of determining  $k$  and  $n$  from the test data would be a least squares fit through many data points. This way errors due to reading either of the two points are minimized.

## II. Step 1

Calculate the reference time  $t_0$  by use of Equations (13) or (14), p. A-7. If the deployment altitude is 50,000 feet or higher, Equation (14) is preferred due to its simplicity. For altitudes from sea level to 50,000 feet, Equation (13) is preferred. Figure 12, p. A-8, shows the effect of altitude on  $t_0$  and can be taken as a guide for the user to decide whether to use Equation (13) or (14). One should keep in mind that the opening shock force can be a strong function of inflation time, so be as realistic as possible. If Equation (13) is elected, the method in use at the NSWC/WO is to program Equation (13) to compute the parachute volume,  $V_0$ , for an assumed value of  $t_0$ . Equation (14), because of its simplicity, can be used for a first estimate of  $t_0$  at all altitudes. The computed canopy volume is then compared to the canopy volume calculated from the geometry of the parachute as per Equation (31), p. A-14. If the volume computed from the mass flow is within the volume computed from the geometry within plus or minus a specified delta volume, the time  $t_0$  is printed out. If not within the specified limits,  $t_0$  is adjusted, and a new volume calculated. For a 35-foot  $D_0$ , T-10 type canopy, I use plus or minus 10 cubic feet in the volume comparison. The limit would be reduced for a parachute of smaller  $D_0$ .

If  $V_0$  calculated =  $V_0$  geometry  $\pm 10$ , then print answer.

If  $V_0$  calculated  $\neq V_0$  geometry  $\pm 10$ , then correct  $t_0$  as follows:

$$t_0 = t_0 \frac{V_0 \text{ geometry}}{V_0 \text{ calculated}} \quad (B-2)$$

The new value of  $t_0$  is substituted in the "do loop" and the volume recomputed. This calculation continues until the required volume is within the specified limits.

III. Calculate  $t_0$  corrected for initial area. The  $t_0$  of Section II assumes that the parachute inflated from a zero initial area. If this is a reasonable assumption for the particular system under study, then the mass ratio can be determined from Equation (6), p. A-4. For  $\eta = 0$  if the value of  $M \leq 0.19$ , then a finite state of deployment exists, and the time ratio of occurrence and the maximum shock factor can be determined from Equations (9) and (10), respectively, on p. A-5. If  $\eta \neq 0$ , then the limiting mass ratio for finite operations will rise slightly as described in Appendix C. Figures C-1 and C-2 illustrate the effects of initial area on limiting mass ratios and shock factors respectively. If the mass ratio is greater than the limiting mass ratio ( $M_L$ ), then the maximum shock force occurs at a time greater than  $t_0$  and the elasticity of the materials must be considered (see Section VI).

If  $\eta \neq 0$ , then the reference time,  $t_0$ , will be reduced, and the mass ratio will rise due to partial inflation at the line stretch. Figures 9 and 10, p. A-6, illustrate the effects of initial area on the velocities and shock factor during the "unfolding" inflation. Equation (15), p. A-9, can be used to correct  $t_0$  calculated for the cases where  $\eta = A_i/A_c$ . If the initial value of drag area is known, Equation (16), p. A-9, can be used to correct  $t_0$  and rechecked for limiting mass ratios versus  $\eta$  in Appendix C.

IV. Opening shock calculations in the elastic phase of inflation. It has been considered that from time  $t = 0$  to  $t = t_0$  the parachute has been inelastic. At the time  $t = t_0$  the applied aerodynamic load causes the materials to stretch and the parachute canopy increases in size. The increased size results in an increase in load, which causes further growth, etc. This sequence of events continues until the applied forces have been balanced by the strength of materials. The designer must insure that the constructed strength of the materials is sufficient to resist the applied loads for the material elongation expected. Use of materials of low elongation should result in lower opening shock forces as  $C_D S_{max}$  is reduced.

When the mass ratio of the system is greater than the limiting mass ratio, the elasticity of the materials and material strength determine the maximum opening shock force. The maximum elongation  $\epsilon_{max}$  and the ultimate strength of the materials are known from tests or specifications. The technique begins on p. A-9.

At the time  $t = t_0$ , calculate the following quantities for the particular values of  $M$  and  $\eta$ .

- a.  $V_0/V_S$  from Equation (18), p. A-9.

- b.  $X_0$  from Equation (22), p. A-10.
- c.  $\epsilon_0$  from Equation (23), p. A-10.
- d. Determine  $C_{DS_{max}}/C_{DS_0}$  from Figure 15, p. A-10.
- e. Calculate the inflation time ratio  $t_f/t_0$  from Equation (24), p. A-10.
- f. Calculate the maximum shock factor from Equation (19), p. A-9.
- g. Calculate the opening shock force  $F_{max.} = X_1 F_s$  where

$$F_s = \frac{1}{2} \rho V_s^2 C_{DS_0}$$

- h. Calculate filling time,  $t_f$ (sec)

$$t_f = t_0 \left( \frac{y}{b} \right)$$

V. In order to simplify the required effort, the work sheets of Table B-1 are included on pages B-5 through B-9 to aid the engineer in systematizing the analysis. The work sheets should be reproduced to provide additional copies.

Table B-1. Opening Shock Force

CALCULATION WORK SHEETS

	SYMBOL	VALUE	DIMENSION
1. Parachute type -			
2. System parameters			
a. System weight, W (lb)		W	lb.
b. Gravity, g (ft/sec <sup>2</sup> )		g	ft/sec <sup>2</sup>
c. Deployment altitude (ft)			ft.
d. Deployment air density, ρ (slugs/ft <sup>3</sup> )		ρ	slugs/ft <sup>3</sup>
e. Velocity at line stretch, V <sub>s</sub> (fps)		V <sub>s</sub>	fps.
f. Steady state canopy data			
(1) Diameter, D <sub>0</sub> (ft)		D <sub>0</sub>	ft.
(2) Inflated diameter, 2ā (ft); $\frac{2\bar{a}}{D_0} = *$		2ā	ft.
(3) Surface area, S <sub>0</sub> (ft <sup>2</sup> ); $\frac{\pi}{4} D_0^2$		A <sub>10</sub> - S <sub>0</sub>	ft. <sup>2</sup>
(4) Drag area, C <sub>D</sub> S <sub>0</sub> (ft <sup>2</sup> ); C <sub>D</sub> x S <sub>0</sub>		C <sub>D</sub> S <sub>0</sub>	ft. <sup>2</sup>
(5) Mouth area, A <sub>MO</sub> <sup>*</sup> (ft <sup>2</sup> )		A <sub>MO</sub>	ft. <sup>2</sup>
$A_{MO} = \pi \bar{a}^2 \left[ 1 - \left( \frac{N/\bar{a} - b/\bar{a}}{b'/\bar{a}} \right)^2 \right]$			
(6) Volume, V <sub>0</sub> <sup>*</sup> (ft <sup>3</sup> )		V <sub>0</sub>	ft. <sup>3</sup>
$V_0 = \frac{2}{3} \pi \bar{a}^3 \left[ \frac{b}{\bar{a}} + \frac{b'}{\bar{a}} \right]$			
g. Cloth data			
(1) k } Calculate using technique beginning on		k	—
(2) n } p. A-12. Note: Permeability is usually measured as ft <sup>3</sup> /ft <sup>2</sup> /min. For these calculations permeability must be expressed as ft <sup>3</sup> /ft <sup>2</sup> /sec		n	—

\* Data for these calculations are listed in Tables 1 and 2, p. A-15.

Table B-1. Opening Shock Force  
(cont'd)

(3)  $\epsilon_{\max}$ ; determine maximum elongations from pull test data of joints, seams, lines, etc. Use minimum  $\epsilon_{\max}$  determined from tests.

(4)  $C_p$ ; pressure coefficient

h. Steady state drag,  $F_s$  (lb),  $F_s = \frac{1}{2} \rho V_s^2 C_D S_o$

i. Parachute constructed strength,  $F_c$  (lb); determined from data on efficiency of seams, joints, lines. Constructed strength is the minimum load required to fail a member times the number of members.

### 3. Force calculations

a. Calculate  $t_o$  for  $\eta = 0$ ; eq. 14, p. A-7.

$$t_o = \frac{14W}{\rho g V_s C_D S_o} \left[ \frac{\rho g V_o}{2W} \left[ \frac{C_D S_o}{A_{MO} - A_{SO} k \left( \frac{C_p \rho}{2} \right)^{\frac{1}{2}}} \right]^{-1} \right]$$

Check Figure 13, p. A-8, for advisability of using eq. 13, p. A-7.

b. If  $\eta = 0$ , proceed with steps c through e. If  $\eta \neq 0$ , go to step f.

c. Mass ratio,  $M$ ; eq. 6, p. A-4

$$M = \frac{2W}{\rho g V_s t_o C_D S_o}$$

d. If  $M \leq 4/21$  for  $\eta = 0$ , then finite mass deployment is indicated.

(1) Time ratio at  $x_{i \max}$ ; eq. 9, p. A-5

$$\frac{t}{t_o @ x_{i \max}} = \left( \frac{21M}{4} \right)^{\frac{1}{7}}$$

(2) Max shock factor,  $x_i$ ; eq., 10, p. A-5

$$x_{i \max} = \frac{16}{49} \left( \frac{21M}{4} \right)^{\frac{6}{7}}$$

SYMBOL	VALUE	DIMENSION
	$C_p$	—
	$F_s$	lb.
	$F_c$	lb.
	$t_o$	sec.
	$M$	—
	$\frac{t}{t_o @ x_{i \max}}$	—
	$x_{i \max}$	—

Table B-1. Opening Shock Force  
(Cont'd)

- (3) Max shock force,
- $F_{\max}$
- (lb)

$$F_{\max} = X_{i \max} F_S$$

e. If  $M > 4/21$ ; then intermediate mass or infinite mass deployment is indicated and the elasticity of materials is involved. Calculate the trajectory conditions at time  $t = t_0$ .

- (1) Velocity ratio @
- $t = t_0$
- for
- $\eta = 0$

$$\frac{V_0}{V_S} = \frac{1}{1 + \frac{1}{7M}}$$

- (2) Shock factor
- $X_0$
- @
- $t = t_0$
- for
- $\eta = 0$

$$X_0 = \frac{1}{\left[1 + \frac{1}{7M}\right]^2} = \left(\frac{V_0}{V_S}\right)^2$$

- (3) Initial elongation,
- $\epsilon_0$
- ; eq. 23, p. A-10

$$\epsilon_0 = \frac{X_0 F_S}{F_c} \epsilon_{\max}$$

- (4) Determine
- $\frac{C_{D S_{\max}}}{C_{D S_0}}$
- from Figure 15, p. A-10

- (5) Calculate inflation time ratio,
- $\frac{t_f}{t_0}$
- ; eq. 24, p. A-10

$$\frac{t_f}{t_0} = \left(\frac{C_{D S_{\max}}}{C_{D S_0}}\right)^{\frac{1}{6}}$$

- (6) Calculate maximum shock factor,
- $X_{i \max}$
- ; eq. 19, p. A-9

$$X_{i \max} = \frac{\left(\frac{t_f}{t_0}\right)^6}{\left[\frac{V_S}{V_0} + \frac{1}{7M} \left[\left(\frac{t_f}{t_0}\right)^7 - 1\right]\right]^2}$$

- (7) Calculate maximum shock force,
- $F_{\max}$
- (lb).

$$F_{\max} = X_{i \max} F_S$$

SYMBOL	VALUE	DIMENSION
	$F_{\max}$	lb.
	$\frac{V_0}{V_S}$	-
	$X_0$	-
	$\epsilon_0$	-
	$\frac{C_{D S_{\max}}}{C_{D S_0}}$	-
	$\frac{t_f}{t_0}$	-
	$X_{i \max}$	-
	$F_{\max}$	lb.

Table B-1. Opening Shock Force  
(cont'd)

	SYMBOL	VALUE	DIMENSION
(8) Inflation time, sec = $t = t_0 \left( \frac{t}{t_0} \right)$		$t$	Sec.
f. If $\eta \neq 0$ , correct $t_0$ for initial area effects; eq. 16, p. A-9		$t_0 = \left[ 1 - \left( \frac{C_D S_i}{C_D S_0} \right)^{1/6} \right] t_0 \text{ calculated}$	Sec.
g. Mass Ratio, M, eq. 6, p. A-4		$M = \frac{2W}{\rho g V_s t_0 C_D S_0}$	-
h. Calculate limiting mass ratio, $M_L$		$M_L = \frac{1}{3(1-\eta)} - \left[ \frac{9}{14} \eta^2 + \frac{3}{14} \eta + \frac{1}{7} \right]$	-
If $M \leq M_L$ , finite mass deployment is indicated and $x_i \text{ max}$ can be determined by eq. 8, p. A-5 by assuming values of $t/t_0$ and plotting the data using the methods of Appendix C.			
i. If $M > M_L$ , then intermediate mass or infinite mass deployment is indicated and the elasticity of materials is involved. Calculate the trajectory conditions at time $t = t_0$ .			
(1) Velocity ratio @ $t = t_0$ for $\eta \neq 0$ ; eq. 18, p. A-9		$\frac{V_0}{V_s} = \frac{1}{\left[ 1 + \frac{1}{M} \left[ \frac{(1-\eta)^2}{7} + \frac{\eta(1-\eta)}{2} + \eta^2 \right] \right]}$	-
(2) Shock factor $X_0$ @ $t = t_0$ for $\eta \neq 0$ ; eq. 22, p. A-10		$X_0 = \frac{1}{\left[ 1 + \frac{1}{M} \left[ \frac{(1-\eta)^2}{7} + \frac{\eta(1-\eta)}{2} + \eta^2 \right] \right]^2} = \left( \frac{V_0}{V_s} \right)^2$	-
(3) Initial elongation, $\epsilon_0$ ; eq. 23, p. A-10		$\epsilon_0 = \frac{X_0 F_s}{F_c} \epsilon_{max}$	-
(4) Determine $\frac{C_D S_{max}}{C_D S_0}$ from Figure 15, p. A-10		$\frac{C_D S_{max}}{C_D S_0}$	-

Table B-1. Opening Shock Force (Contd)

- p. A-10 (5) Calculate inflation time ratio,  $\frac{t_f}{t_o}$ ; eq. 24,

$$\frac{t_f}{t_o} = \left( \frac{C_D S_{max}}{C_D S_o} \right)^{\frac{1}{6}}$$

 $\frac{t_f}{t_o}$ 

-

- eq. 19, p. A-9 (6) Calculate maximum shock factor,  $x_{i \max}$ ;

$$x_{i \max} = \frac{\left( \frac{t_f}{t_o} \right)^6}{\left[ \frac{V_s}{V_o} + \frac{1}{7M} \left[ \left( \frac{t_f}{t_o} \right)^7 - 1 \right] \right]^2}$$

 $x_{i \max}$ 

-

- (7) Calculate maximum shock force,  $F_{\max}$ (lb)

$$F_{\max} = x_{i \max} F_s$$

 $F_{\max}$ 

lb.

- (8) Calculate inflation time,  $t_f$ (sec)

$$t_f = t_o \left( \frac{t_f}{t_o} \right)$$

 $t_f$ 

Sec.

## DISTRIBUTION

	<u>Copies</u>		<u>Copies</u>
Commander Naval Air Systems Command Attn: Library Department of the Navy Washington, DC 20361	4	Commander Naval Air Development Center Attn: Library William B. Shope David N. DeSimone Louis A. Daulerio Thomas J. Popp Maria C. Hura Warminster, PA 18974	2 1 1 1 1 1
Commander Naval Sea Systems Command Attn: Library Washington, DC 20362	4	Commanding Officer Naval Weapons Support Center Attn: Library Mark T. Little Crane, IN	2 1
Commanding Officer Naval Personnel Research and Development Center Attn: Library Washington, DC 20007	2	Commander Naval Ship Research and Development Center Attn: Library Washington, DC 20007	2
Office of Naval Research Attn: Library Washington, DC 20360	4	Commander Pacific Missile Test Center Attn: Technical Library, Code NO322 Point Mugu, CA 93041	2 2
Office of Naval Research Attn: Fluid Dynamics Branch Structural Mechanics Branch 800 N. Quincy St. Arlington, VA 22217	2	Director Marine Corps Development and Education Command Development Center Attn: Library Quantico, VA 22134	2
Director Naval Research Laboratory Attn: Code 2027 Library, Code 2029 (ONRL) Washington, DC 20375	2	Marine Corps Liaison Officer U.S. Army Natick Laboratories Natick, MA 01760	2
U.S. Naval Academy Attn: Library Annapolis, MD 21402	2		
Superintendent U.S. Naval Postgraduate School Attn: Library (Code 0384) Monterey, CA 93940	2		

## DISTRIBUTION (Cont.)

<u>Copies</u>	<u>Copies</u>
Commanding General U.S. Army Mobility Equipment Research and Development Center Attn: Technical Document Center Fort Belvoir, VA 22660	2     2
Commanding General U.S. Army Aviation Systems Command Attn: Library St. Louis, MO 63166	2     2
Commanding General U.S. Army Munitions Command Attn: Technical Library Stanley D. Kahn Dover, NJ 07801	2   1   2
Commanding General U.S. Army Weapons Command Attn: Technical Library Research and Development Directorate Rock Island, IL 61201	2      2
Commanding General U.S. Army ARDEC Attn: Library Walt Koenig, SMCAR-AET-A Roy W. Kline, SMCAR-AET-A Dover, NJ 07801	2  1  1   2
Army Research and Development Laboratories Aberdeen Proving Ground Attn: Technical Library, Bldg. 313 Aberdeen, MD 21005	2     2
Commanding General Edgewood Arsenal Headquarters Attn: Library Aero Research Group Aberdeen Proving Ground Aberdeen, MD 21005	2     2
Commanding General Harry Diamond Laboratories Attn: Technical Library 2800 Powder Mill Road Adelphi, MD 20783	2     2
U.S. Army Ballistic Research Laboratories Attn: Technical Library Aberdeen Proving Ground Aberdeen, MD 21005	2     2
Commanding General U.S. Army Foreign Science and Technology Center Attn: Technical Library 220 Seventh Street, NE Federal Building Charlottesville, VA 22312	2      2
Commanding General U.S. Army Materiel Command Attn: Library Washington, DC 20315	2     2
Commanding General U.S. Army Test and Evaluation Command Attn: Library Aberdeen Proving Ground Aberdeen, MD 21005	2     2
Commanding General U.S. Army Combat Developments Command Attn: Library Fort Belvoir, VA 22060	2     2
Commanding General U.S. Army Combat Developments Command Attn: Technical Library Carlisle Barracks, PA 17013	2     2
Commanding General U.S. Army Materiel Laboratories Attn: Technical Library Fort Eustis, VA 23604	2     2

## DISTRIBUTION (Cont.)

	<u>Copies</u>		<u>Copies</u>
U.S. Army Air Mobility R&D Laboratory Eustis Directorate Attn: Systems and Equipment Division Fort Eustis, VA 23604	2	U.S. Army Advanced Material Concepts Agency Department of the Army Attn: Library Washington, DC 20315	2
President U.S. Army Airborne Communications and Electronic Board Fort Bragg, NC 28307	2	Director U.S. Army Mobility R&D Laboratory AMES Research Center Attn: Library Moffett Field, CA 94035	2
U.S. Army CDC Institute of Land Combat Attn: Technical Library 301 Taylor Drive Alexandria, VA 22314	2	Commandant Quartermaster School Airborne Department Attn: Library Fort Lee, VA 23801	2
Commanding General Frankford Arsenal Attn: Technical Library Bridge and Tacony Streets Philadelphia, PA 19137	2	U.S. Army Standardization Group, UK Attn: Research/General Material Representative Box 65 FPO, NY 09510	2
Commanding General U.S. Missile Command Redstone Scientific Information Center Attn: Library Redstone Arsenal, AL 35809	2	Commanding Officer McCallan AFB Attn: Library SA-ALC/MMIR McCallan AFB, CA 95652	2
U.S. Army Natick Laboratories Liaison Office Attn: Library Aeronautical Systems Division Wright Patterson AFB, OH 45433	2	Arnold Engineering Development Center (ARO, Inc.) Attn: Library/Documents Arnold Air Force Station, TN 37389	2
Army Research Office Attn: Library Box CM, Duke Station Durham, NC 27706	2	NASA Lewis Research Center Attn: Library, Mail Stop 60-3 21000 Brookpark Road Cleveland, OH 44135	1
Office of the Chief of Research and Development Department of the Army Attn: Library Washington, DC 20310	2	NASA John F. Kennedy Space Center Attn: Library, Code IS-CAS-42B Kennedy Space Center, FL 32899	1

## DISTRIBUTION (Cont.)

	<u>Copies</u>		<u>Copies</u>
NASA Manned Spacecraft Center Attn: Library, Code BM6 2101 Webster Seabrook Road Houston, TX 77058	1	Defense Technical Information Center Cameron Station Alexandria, VA 22314	12
NASA Marshall Space Flight Center Attn: Library Huntsville, AL 25812	1	Library of Congress Attn: Gift and Exchange Division Washington, DC 20540	4
NASA Goddard Space Flight Center Wallops Island Flight Facility Attn: Library	2	University of Minnesota Dept. of Aerospace Engineering Attn: Dr. W. L. Garrard	2
Mr. Mendle Silbert	1	Minneapolis, MN 55455	
Mr. Earl B. Jackson, Code 841.2	1	Sandia National Laboratories Attn: Code 1632	2
Mr. Dave Molledo, Code 841.2	1	Library	2
Mr. Anel Flores	1	Dr. Dean Wolf	1
Wallops Island, VA 23337		Dr. Carl Peterson	10
National Aeronautics and Space Administration		R. Kurt Baca	1
Attn: Library	2	Ira T. Holt	1
Headquarters, MTG		Donald W. Johnson	1
400 Maryland Avenue, SW		James W. Purvis	1
Washington, DC 20456		Harold E. Widdows	1
Defense Advanced Research Projects Agency		Albuquerque, NM 87185	
Attn: Technical Library	2	Applied Physics Laboratory The Johns Hopkins University Attn: Document Librarian	2
1400 Wilson Boulevard		Johns Hopkins Road	
Arlington, VA 22209		Laurel, MD 20810	
Director Defense Research and Engineering		National Academy of Sciences National Research Council / Committee on Undersea Warfare	
Attn: Library (Technical)	2	Attn: Library	2
The Pentagon		2101 Constitution Ave., N.W.	
Washington, DC 20301		Washington, DC 20418	
Director of Defense Research and Engineering	2	Sandia Corporation Livermore Laboratory	
Department of Defense		Attn: Technical Reference Library	2
Washington, DC 20315		P. O. Box 969 Livermore, CA 9455	

## DISTRIBUTION (Cont.)

Copies

Lockheed Missiles and Space Co.  
 Attn: Mr. K. French 1  
 P.O. Box 504  
 Sunnyvale, CA 94086

Rockwell International Corporation  
 Space and Information Systems Div.  
 Attn: Technical Information Center 2  
 12214 S. Lakewood Boulevard  
 Downey, CA 90241

Pennsylvania State University  
 Applied Research Laboratory  
 Attn: Library 2  
 P.O. Box 30  
 State College, PA 16801

Honeywell, Incorporated  
 Attn: M. S. Sopczak 1  
 600 Second Street N.  
 Hopkins, MN 55343

National Bureau of Standards  
 Attn: Library 2  
 Washington, DC 20234

Internal Distribution:  
 U13 (C. J. Diehlmann) 1  
 U13 (W. P. Ludtke) 25  
 U13 (J. F. McNelia) 1  
 U13 (D. W. Fiske) 1  
 U13 (J. Murphy) 1  
 U13 (J. G. Velez) 1  
 U13 (M. L. Fender) 1  
 U13 (R. L. Pense) 1  
 U13 (M. L. Lama) 1  
 U43 (J. Rosenberg) 1  
 U43 (B. Delre) 1  
 E231 9  
 E232 3  
 E31 (GIDEP) 1

**SUPPLEMENTARY**

**INFORMATION**



DEPARTMENT OF THE NAVY  
NAVAL SURFACE WEAPONS CENTER  
DAHLGREN, VIRGINIA 22448-6000

WHITE OAK  
10981 NEW HAMPSHIRE AVE.  
SILVER SPRING, MD. 20903-5000  
(202) 394-4404

DAHLGREN, VA. 22448-6000  
(703) 863-

IN REPLY REFER TO:

E221-MEM

Change 1

To all holders of  
Title:

NSWC TR 87-96  
Notes on a Parachute Opening Force Analysis  
Applied to a Vertical Toward-the-Earth  
Trajectory

17 Jul 87

3 page(s)

This publication is changed as follows:

Remove the following pages and replace with new pages supplied:

13/14

Insert the following new pages supplied:

13/14

Dispose of the removed pages in accordance with applicable security regulations.

Insert this change sheet between the cover and the DD Form 1473 in your copy.  
Write on the cover "Change 1 inserted"

Approved by:

*J. E. Goeller*  
DR. J. E. GOELLER, Head  
Underwater Weapons Division

87 10 1 366

AD-A180901

The calculated canopy volume,  $V_o$  calc, is determined from equation (11).

$$V_{o\text{calc}} = \int_{V=0}^{V_o} dV = \int_{t=0}^{t_o} \left[ VA_{mo} \left( \frac{t}{t_o} \right)^6 - A_{so} \left( \frac{t}{t_o} \right)^6 k \left( \frac{C.P.\rho}{2} \right)^n v^{2n} \right] dt \quad (11)$$

A program for calculating  $t_o$  for solid cloth parachutes and the opening shock force profile during the inflation of several parachute types is provided in Table 1. Equations (4), (11), and (12) are programmed together with the vertical deployment opening shock equations (2) through (8) in FORTKAN IV language. The included examples were calculated via the program using a VAX 780 computer. The program operates in two modes. Mode 1, for solid cloth parachutes, calculates the vertical deployment reference time  $t_o$  for the parachute system parameters and operational deployment data, and then calculates the opening shock profile during inflation. A typical data print out is shown in Table 2. It is necessary to estimate an initial value of " $t_o$ ". The program calculates the canopy volume for the estimated time and compares the  $V_o$  calc to the volume derived from the canopy geometry. If the calculated volume is not within specified limits, the program adjusts " $t_o$ " by equation (12) and reiterates the program until the calculated volume is within the specified limits.

$$t_o = t_o \left( \frac{V_o \text{ geometric}}{V_o \text{ calc.}} \right) \quad (12)$$

Mode 2 of the program calculates opening shock profiles for input values of  $t_o$ . Mode 2 analysis of other types of parachutes is possible by the selection of the proper values of "j" (1/2, 1, 2, 3, 4, 5, or 6) and " $\tau$ ". The opening shock force variation for examples (1) and (2) are plotted in Figures 3 and 4. The nominal  $t_o$  for  $n=0.632$  was calculated by the program in mode 1 and the force-time survey was calculated in mode 2.

Figure 3 illustrates that parachutes deployed in a vertical toward-the-earth trajectory inflate faster than the same system deployed horizontally at the same altitude and velocity.

Inflation reference times for parachute types other than solid cloth canopies can be developed from the mass flow equation. This requires that the flow through the canopy be expressed in a form similar to the solid cloth canopy cloth permeability, P, where the rate of flow per unit area is a function of the pressure differential across the cloth or grid.

NSWC TR 87-96

TABLE 1. INSTANTANEOUS DRAG AREA, VELOCITY, OPENING SHOCK FORCE, AND DISTANCE OF FALL OF A PARACHUTE DEPLOYED IN VERTICAL FALL.

THIS PROGRAM CALCULATES THE INSTANTANEOUS DRAG AREA, VELOCITY, OPENING SHOCK FORCE, AND DISTANCE OF FALL OF A PARACHUTE DEPLOYED IN VERTICAL FALL.

THE PROGRAM OPERATES IN TWO MODES:

- MODE 1 - CALCULATES THE INFLATION TIME AND PERFORMANCE PROFILES FOR SOLID CLOTH PARACHUTES (TO INPUT AS INITIAL ESTIMATE) (IOPT = 1)
- MODE 2 - CALCULATES THE PERFORMANCE PROFILES FOR VARIOUS TYPES OF PARACHUTES (J). INFLATION TIME INPUT IS REQUIRED (IOPT = 2)

INPUT: IOPT - 1 (FOR MODE 1)  
 - 2 (FOR MODE 2)

INPUT NEEDED FOR BOTH MODES:

- RHO - AIR DENSITY AT GIVEN ALTITUDE (SLUGS/FT<sup>3</sup>)
- VS - VELOCITY AT SUSPENSION LINE STRETCH (FT/SEC)
- CDSO - DESIGN DRAG AREA (FT<sup>2</sup>)
- TO - IOPT=1 INITIAL GUESS FOR INFLATION REF. TIME (SEC)  
 IOPT=2 ACTUAL INFLATION REFERENCE TIME (SEC)
- W - WEIGHT (LBS)
- J - =6 FOR FLAT CIRCULAR PARACHUTE  
 =1 FOR RIBBON TYPE OF PARACHUTE

INPUT NEEDED FOR IOPT = 1 ONLY:

- AMO - STEADY-STATE MOUTH AREA (FT<sup>2</sup>)
- ASO - CANOPY DESIGN SURFACE AREA (FT<sup>2</sup>)
- K - CLOTH PERMEABILITY CONSTANT
- CP - PRESSURE COEFFICIENT
- N - CLOTH PERMEABILITY EXPONENT
- VO - GEOMETRIC VOLUME (FT<sup>3</sup>)

```

REAL*4 N
TODEN=100000
5 PRINT *, 'INPUT IOPT'
READ(5, *, END=100) IOPT
PRINT *, 'INPUT RHO, VS, CDSO, TO, W, J'
READ(5, *) RHO, VS, CDSO, TO, W, J
IF (IOPT.EQ.2) GO TO 3
PRINT *, 'INPUT AMO, ASO, XK, CP, N, VO'
READ(5, *) AMO, ASO, XK, CP, N, VO
3 DT=TO/TODEN
TAU=0.
Q=32.2
S=0.
X=TAU
CDS=TAU*CDSO
FS=.5*RHO*VS**2*CDSO
F=TAU*FS
VOL=0
IPASS=0
  
```